1 Title and Authors:

The nitrogen cycle: a review of isotope effects and isotope modeling approaches

Tobias R. A. Denk[1,5], Joachim Mohn[2,6], Charlotte Decock[3,7], Dominika Lewicka-Szczebak[4,8], Eliza Harris[2,9], Klaus Butterbach-Bahl[1,10], Ralf Kiese[1,11], Benjamin Wolf[1,12]

[1]Karlsruhe Institute of Technology, Institute for Meteorology and Climate Research, Atmospheric Environmental Research (IMK-IFU), Kreuzeckbahnstrasse 19, Garmisch-Partenkirchen 82467, Germany

[2]Laboratory for Air Pollution & Environmental Technology, Empa, Überlandstr. 129, 8600 Dübendorf, Switzerland

[3]Department of Environmental System Science, ETH-Zurich, Tannenstrasse 1, 8092 Zurich, Switzerland

[4]Thünen Institute of Climate-Smart Agriculture, Federal Research Institute for Rural Areas, Forestry and Fisheries, Bundesallee 50, 38116 Braunschweig, Germany

[5]Correspondence: T. R. A. Denk. E-mail: tobias.denk@kit.edu

[6]E-mail: Joachim.Mohn@empa.ch

[7]E-mail: charlotte.decock@usys.ethz.ch

[8]E-mail: dominika.lewicka-szczebak@ti.bund.de

[9]E-mail: Eliza.Harris@empa.ch

[10]E-mail: klaus.butterbach-bahl@kit.edu

[11]E-mail: ralf.kiese@kit.edu

[12]E-mail: benjamin.wolf@kit.edu

Keywords: Nitrogen cycle; Isotopes; 15N; Isotope modelling; Fractionation; Isotope effect

2 Abstract

The nitrogen (N) cycle involves a set of N compounds transformed by plants and microbes. Some of these N compounds, such as nitrous oxide (N_2O) or nitrate (NO_3^-), are environmental pollutants jeopardizing biodiversity, human health or the global climate. The natural abundances of the common (^{14}N) and rare (^{15}N) stable N isotopes in a given compound, i.e. the isotopic composition, depend on individual production and consumption processes. As each process has an individual preference for the common or rare isotope (isotope effect) the measurement of the isotopic composition has been identified as a powerful tool for improved process understanding and source process identification. Both are key requirements for the development of strategies aiming at mitigating the release of environmental harmful N compounds. However, up to now, no comprehensive compilation of N cycle isotope effects is available.

A compilation of isotope effects is also in high demand for testing biogeochemical models as such models are increasingly used to study N cycling in ecosystems and across landscapes and regions. Biogeochemical models are usually calibrated and validated only with single, easily accessible quantities. The isotopic composition of N compounds has a high potential to be used as additional, integrative parameter for a more thorough assessment of simulation results. For instance, the isotopic composition of soil N is determined by fractionation of the most relevant processes and, thus, integrates several N cycle processes, some of which cannot be accessed easily by direct measurement. To implement isotopic fractionation in ecosystem models and to utilize those for model validation, the magnitude of the isotope effects associated with individual transformations in the N cycle need to be assessed.

This review summarizes the available methods to determine N isotope effects of various key ecosystem processes, thereby systematically comparing isotope effects for different experimental conditions and processes, exploring the accuracy of theoretical calculations of isotope effects and finally, addressing concepts to implement isotope effects into biogeochemical modeling.

Our review shows that published isotope effects for N processes in soil incubations seem to be stronger as compared to those in water saturated systems. In addition to the choice of isotope effects adequate for the respective ecosystem, the challenge for modeling approaches is the sequential calculation of isotopic compositions. Associated numerical inaccuracies can be minimized by controlling the share of reacted substrates, i.e. the time step. The criterion to determine the time step needs to consider the strongest isotope effect, required accuracy of the calculations and the share of substrate consumed from or provided to the compound pool.

The combination of biogeochemical models with $\delta^{15}N$ methods and novel measures like site preference (SP) of N_2O is a promising approach for improving process understanding at various spatial and temporal scales. Nevertheless, the compilation of isotope effects in this review may not only be of benefit for modelers, but also for experimentalists, as measurement and modelling of isotope effects may eventually help to test and validate our current process understanding of the N cycle.

3 Introduction

As essential compound of the DNA, proteins or enzymes, nitrogen (N) is a key component of life and a fundamental nutrient. Its most abundant form, atmospheric dinitrogen (N_2), is unavailable for most organisms, making nitrogen a limiting nutrient (Galloway et al., 2003; Vitousek and Howarth, 1991). Therefore, the conversion of N_2 into reactive nitrogen (N_r) directly or indirectly supports biomass growth. In the environmental context, reactive nitrogen compounds include oxidized nitrogen species,

63 such as nitric oxide (NO), nitrogen dioxide (NO_2), nitrous oxide (N_2O), nitrate (NO_3^-), nitrite (NO_2^-) as well
64 as the reduced nitrogen species, ammonia (NH_3) and ammonium (NH_4^+) salts, as well as organic bound N
65 e.g. in its simplest form of urea, amine derivatives or as organic N in proteins or other substances. The
66 main natural processes creating biologically available N_r are lightning (globally approx. 5 Tg N yr^{-1}) and
67 biological N_2-fixation (BNF) in terrestrial and aquatic ecosystems (globally approx. 198 Tg N yr^{-1}) (Fowler
68 et al., 2013). However, in most ecosystems the demand of N_r by far exceeds natural N_2-fixation by both
69 processes, so that ecosystems are in general N limited (Aber et al., 1989). This shortage was revoked
70 following the invention of the Haber-Bosch process, which allowed to convert N_2 into NH_3/NH_4^+ at
71 industrial scale (Erisman et al., 2008) and was used at the beginning for the production of explosives
72 with the focus changing in the following to the production of synthetic fertilizers. The increasing use of
73 synthetic N fertilizers in the mid of the last century boosted global agricultural production and allowed
74 to sustain an ever growing world population, with approx. 50% of the global world population currently
75 being fed due to the availability of the Haber-Bosch technology (Erisman et al., 2008). However, the use
76 and overuse of N fertilizers is also associated with detrimental effects on the terrestrial and aquatic
77 environment, climate and human health as N_r is driving eutrophication (increasing mineral and organic N
78 in ecosystems), acidification (as a consequence of oxidizing NH_4^+ to NO_3^-), radiative forcing (mainly by
79 the greenhouse gas N_2O), stratospheric ozone depletion (stratospheric degradation of N_2O to NO with
80 the latter acting as O_3 depleting substance), tropospheric ozone production (due to soil emissions of NO
81 and its chemical reactions in the troposphere) and $PM_{2.5}$ formation (as e.g. NH_4NO_3 is a major particle
82 forming substance) (for a detailed overview see Galloway et al. (2003) or Fowler et al. (2013) and
83 references therein).

84 Due to the delicate coexistence of beneficial and detrimental effects, a profound understanding of N
85 cycle processes is required to develop efficient mitigation strategies sustaining agricultural productivity
86 (Butterbach-Bahl et al., 2013). The fundamental process in N cycling is *nitrogen fixation*: The conversion

of atmospheric N_2 to NH_3 by nitrogen-fixing microorganisms which oxidize ("burn") carbohydrates to gain energy and thereby reduce N_2 to NH_3 (biological nitrogen fixation). Once fixed, N is transformed to microbial or plant biomass (*immobilization and uptake, respectively*), eventually ending up in the soil organic matter pool (SOM) after senescence, littering and decomposition. Microbes are involved in a process called *mineralization*, which represents the breakdown of complex organic matter molecules into monomeric organic nitrogen compounds *(depolymerization)* and inorganic NH_4^+ (Schimel and Bennett, 2004). NH_4^+ can be utilized by microbes to gain energy in a two-step process called *nitrification*. In the first step, $NH4^+$ is oxidized to NO_2^- via the intermediate hydroxylamine (NH_2OH); in the second step NO_2^- is oxidized to NO_3^-. Both reactions can be carried out by chemo-lithotrophic ammonium or nitrite oxidizers. However, also heterotrophic bacteria, fungi and archaea might be capable to nitrify, though without gaining energy from the process, thereby using monomeric organic nitrogen compounds for growth. NO_3^- can be lost to ground water through leaching and at high pH NH_4^+ can *volatilize* and be lost to the atmosphere in gaseous form as NH_3. In the anoxic process of *denitrification*, NO_3^- is used as alternative electron acceptor instead of O_2, and be stepwise reduced via NO_2^-, NO and N_2O to N_2. Two other notable processes are *dissimilatory nitrate reduction to ammonium* (DNRA), during which NO_3^- is reduced to NO_2^- and then transformed to NH_4^+ and N_2O, as well as *anaerobic ammonia oxidation* (ANAMMOX) producing N_2 from both NH_4^+ and NO_2^- (Harris et al., 2015). Additionally to these biotic processes in soils, also *abiotic N_2O production* can happen in soils with the nitrification byproducts NH_2OH and NO_2^- as substrate (Bremner, 1997) (see Figure 1).

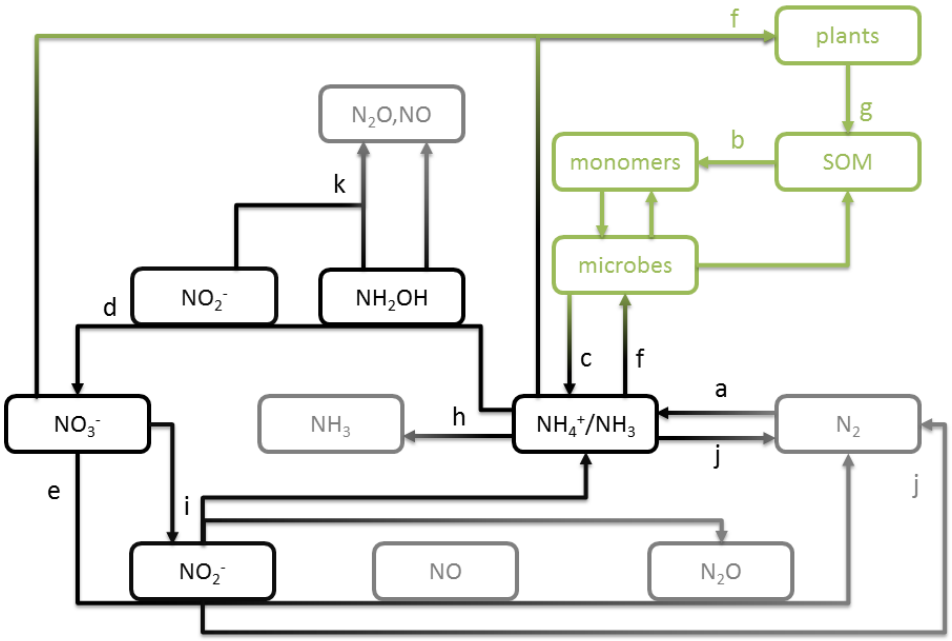

Figure 1: Processes involved in terrestrial ecosystem N cycling: a) biological N_2 fixation, b) depolymerization, c) mineralization, d) nitrification, e) denitrification, f) immobilization and plant uptake, g) senescence, h) volatilization, i) dissimilatory nitrate reduction to ammonium, j) anaerobic ammonia oxidation, k) abiotic N_2O production. Soil N compounds are shown in black, gaseous compounds in grey and organic N in green.

N transformation processes in aquatic and terrestrial ecosystems have been studied extensively from laboratory to global scales by means of various different measuring approaches (e.g., microbial pure culture experiments, analysis of N_r concentrations and fluxes) including isotope techniques (Bai et al., 2012; Groffman et al., 2006; Houlton et al., 2015). Experimental techniques are supported by modelling approaches, which assess environmental impacts of N cycling on regional and global scale using process-oriented biogeochemical models like O-CN (Zaehle and Friend, 2010; Zaehle et al., 2010), LandscapeDNDC (Haas et al., 2013), DAYCENT (Del Grosso et al., 2000), PASIM (Riedo et al., 1998) or the Coup Model (Jansson and Moon, 2001), which consider relevant processes involved in N and C transformations. Further, these models are used to develop efficient mitigation strategies for reducing soil emissions of N_2O (e.g. Molina-Herrera et al. (2016)) and can consider impacts of climate change on ecosystem N cycling and soil N_2O and NO emissions (Kesik et al., 2005). However, validation of these

models is usually restricted to single quantities, such as biomass production, crop yields, soil nitrogen concentrations or the emissions of environmental important nitrogen trace gases such as N_2O (a direct GHG) or NO (an indirect GHG due to its key contributions to tropospheric O_3 formation). Hence, a more integrated model validation considering contributing N processes (e.g. ammonification, nitrification, and denitrification) is pertinent.

As biological and physico-chemical N transformation processes are associated with different degrees of isotopic fractionation, the isotopic composition of soil and plant nitrogen compounds can provide information on the predominant processes and can, thus, be considered as an integrating measure (Robinson, 2001). For instance this potential has been demonstrated at six tropical forest sites in Hawaii (USA), where decreasing soil ^{15}N enrichment was observed along a rainfall gradient of 2200 mm to 5050 mm (Houlton et al., 2006). Isotopic analysis of N compounds indicated that the observed pattern could not be explained by the isotopic composition of N inputs or preferential leaching of ^{14}N to streams, but by the dominance of gaseous N losses via denitrification which was highest at sites receiving highest precipitation amounts.

For this reason, implementation of isotopic composition of N compounds in biogeochemical models and global carbon-nitrogen models may advance our understanding of the N cycle and provide a further, integrative constraint for the validation of these models (see e.g. Houlton et al. (2015)). A first successful example is the integration of isotope calculation in the process-oriented model DAYCENT (Bai and Houlton, 2009). Emerging N isotope techniques will further extend the range of reaction pathways and nitrogen compounds which can be analyzed and implemented into models. E.g. Intra molecular N_2O isotopic composition and the quantity site preference, SP, i.e. the difference in ^{15}N substitution in the central and terminal position of the linear N_2O molecule (Brenninkmeijer and Röckmann, 1999; Toyoda and Yoshida, 1999), has been identified as powerful indicator to identify underlying source processes

(source partitioning) of soil N_2O emissions. Two examples of the use of emerging N isotope techniques are the first semi-continuous field measurements of intra molecular N_2O isotopic composition (Mohn et al., 2012; Wolf et al., 2015) and the selective analysis of δ^{15}N-NH_4^+, -NO_2^- and -NO_3^- by automated sample preparation of the inorganic nitrogen species coupled to a quadrupole mass spectrometer (Stange et al., 2007). However, the successful integration of N isotopic composition into models requires first a comprehensive database of isotope effects and secondly its uncertainty quantification for main N cycle processes, which is not yet available.

To foster the fusion of modeling and isotope techniques this work:

i. gives an overview of the methods used to derive N isotope effects,
ii. reviews available information on isotope effects for different microbial, plant and physico-chemical N processes and compares the methods used to derive them,
iii. considers theoretical calculation of isotopic N fractionation factors for processes underrepresented in the literature,
iv. summarizes isotope calculation concepts for time-discrete mathematical modelling.

4 Isotope calculations

Multiple stable isotopes exist for most chemical elements and N specifically has two stable isotopes with the atomic masses 14 (^{14}N) and 15 (^{15}N). The isotopic composition of a sample is described using the δ-notation given in equation (1) (Coplen, 2011):

$$\delta^{15}N = R_{sample}/R_{standard} - 1, \quad (1)$$

R denotes the isotope ratio ^{15}N/^{14}N. The δ^{15}N value of a sample is therefore the deviation of the sample's ^{15}N/^{14}N isotope ratio from the respective isotope ratio of the reference material (AIR-N_2 for N) and is usually expressed in ‰.

4.1 Fractionation and mixing

Although isotopes of an element, e.g. ^{15}N or ^{14}N, display similar physico-chemical properties, their relative abundance (isotope ratio) varies between different N compounds. This is the consequence of isotope fractionation which arises from stronger chemical bonds formed by heavier isotopes or from mass-dependent processes such as diffusion (Farquhar et al., 1989). In other words, the substitution of an atom in a reactant molecule by one of its isotopes alters either the equilibrium constant K or the reaction rate k. This alteration is referred to as the thermodynamic (equilibrium) isotope effect or kinetic (non-equilibrium) isotope effect, respectively (Coplen, 2011). Examples are CO_2-fixation in plants for the unidirectional kinetic isotope effect and the two-way exchange of air CO_2 with ocean bicarbonate for the equilibrium isotope effect (Fry, 2006), with denitrification and ammonia volatilization representing respective N cycle processes. The isotopic fractionation factor $\alpha_{p/s}$ is defined as the ratio of isotope ratios of the instantaneously formed product R_{pi} and substrate, R_s, and can be interpreted as the ratio of rate constants *k* or equilibrium constants K for ^{15}N and ^{14}N; eq. (2).

$$\alpha_{p/s} = \frac{^{15}k}{^{14}k} = \frac{^{15}K}{^{14}K} \qquad (2)$$

In this definition, $\alpha_{p/s}$ is smaller than 1 for the normal isotope effect, where the lighter isotope reacts faster than the heavier isotope in a unidirectional kinetic reaction. In the literature the isotopic fractionation factor is often reported as inverse convention $\alpha_{s/p}$, where the normal isotope effect is larger than 1. The two notations can be converted into each other by inversion of α ($\alpha_{p/s} = 1/\alpha_{s/p}$). Differences in isotopic fractionation factors are often very small and therefore, the isotope effect ε = (α - 1), is given in per mille for more convenient comparability of values. All isotope effects summarized in this study were recalculated to comply with the sign convention of $\alpha_{p/s}$.

While the above formulations assume single step reactions, biological processes or elemental cycles may involve reaction sequences. Denitrification, a fundamental process in the N cycle (section 3) for instance,

188 is a microbial process that comprises the diffusion of NO_3^- into the microbial organism followed by the
189 reduction of NO_3^- to N_2 via the intermediates NO_2^-, NO and N_2O. Each of the single reactions will have its
190 own intrinsic isotopic fractionation factor, which may not always be accessible to measurements. Thus,
191 isotope effects observed for complex reactions with several intermediates are apparent or net isotope
192 effects (η) (Ostrom and Ostrom, 2011). The probably most prominent example for a model describing η
193 is available for photosynthesis; eq. (3).

$$\eta = \varepsilon_a + (\varepsilon_b - \varepsilon_a)K_1/(K_2 + K_3) \qquad (3)$$

194 It involves the intrinsic isotope effects for diffusion (ε_a), enzymatic reaction (ε_b), and the relative rates of
195 diffusion into the cell (K_1), out of the cell (K_2) and of the enzymatic reaction (K_3). This formulation is
196 capable of reflecting apparent isotope effects that are observed if diffusion into the cell limits substrate
197 availability for the enzymatic processes and leads to a complete conversion of the substrate in the cell
198 (i.e., $K_2+K_3 \gg K_1$ for which $\eta \approx \varepsilon_a$), while η reaches the stronger isotope effect of the enzymatic reaction,
199 ε_b, if diffusion into the cell is not limiting (Farquhar et al., 1982). Since all measured isotope effects are
200 apparent we refer to them as net isotope effect or η.

201 The change in isotopic composition of a pool of a given N compound is not only determined by
202 fractionation, but may also depend on the mixture of different processes yielding or drawing on the
203 respective compound. Hence, mixing of a given N compound originating from different source processes
204 (i.e. isotope mass balance) and/or transport processes need to be considered in addition to fractionation
205 processes. To calculate the evolution of the isotopic composition of both reaction product and
206 substrate, different approaches are frequently used in the reviewed literature. These involve different
207 assumptions on the system boundaries and differ in the amount of parameters used. The most
208 prominent approaches are the closed and the open system approaches summarized in the next two
209 sections as they represent the basis for the experimental determination of isotope effects.

4.2 Closed system approach

The closed system approach considers an isolated system that does not exchange substances with its surroundings, e.g. gaseous losses or leaching losses of N compounds do not occur and no additional N_r is added. The methods to calculate fractionation processes in closed systems were developed by Mariotti et al. (1981). The derivation is based on the definition of the isotopic fractionation factor

$\alpha_{p/s} = \frac{R_{pi}}{R_s}$	(4)

as well as the approximation that the remaining fraction of substrate can be described as $f = N_s/N_{s,0} \approx {}^{14}N_s/{}^{14}N_{s,0}$ and yields the Rayleigh equations (Mariotti et al., 1981):

$R_s = R_{s,0}\, f^{(\alpha_{p/s}-1)}$	(5)
$R_{pi} = \alpha_{p/s} * R_{s,0}\, f^{(\alpha_{p/s}-1)}$	(6)
$R_p = R_{s,0}\frac{1-f^{\alpha_{p/s}}+R_{s,0}(f^{\alpha_{p/s}-1}-f)}{1-f+R_{s,0}(f^{\alpha_{p/s}-1}-f)} \approx R_{s,0}\frac{1-f^{\alpha_{p/s}}}{1-f}.$	(7)

Equations (5) to (7) describe the evolution of the isotope ratio of the remaining substrate, instantaneous product and accumulated product (R_s, R_{pi} and R_p, respectively). It is a function of the initial substrate isotope ratio $R_{s,0}$, the fraction of remaining substrate f and of the isotopic fractionation factor $\alpha_{p/s}$ of the process. Using the assumption that δ-values are small, several relations between the δ-values in product and substrate can be derived. These relate the δ-values of the substrate δ_s (8), the accumulated product δ_p (9) and the instantaneous product δ_{pi} (10) to the isotope effect, knowing the fraction of remaining substrate and the isotopic composition of the initial substrate (Mariotti et al., 1981):

$\delta_s - \delta_{s,0} \approx \varepsilon\, ln(f)$	*(8) referred to as method S*
$\delta_p - \delta_{s,0} \approx -\varepsilon\frac{f*ln(f)}{(1-f)}$	*(9) referred to as method P*

$\delta_{pi} - \delta_s \approx \varepsilon$	*(10) referred to as method Δ*

Equations (8) to (10) are frequently used to derive isotope effects. For the sake of clarity, we refer to methods S, P and Δ in situations in which the isotope effect was calculated by solving equations (8) to (10), respectively for ε (see section 4.5). An alternative formalism treating the closed system and specifically aiming at the determination of isotope effects was introduced by Tong and Yankwich (1957). The derivation is based on pseudo first-order reaction systems for both ^{14}N and ^{15}N. Four equations were derived with each one describing the isotopic fractionation factor as a function of three of the quantities $R_{s,0}$, R_s, R_p and f. The equation involving R_s, R_p and f was used in two studies presented in this review and is given in eq. (11).

$\frac{1}{\alpha_{p/s}} = \frac{\ln\left(\frac{1}{f} - \frac{(1-f)(R_p - R_S)}{f(R_p+1)}\right)}{\ln\left(\frac{1}{f} - \frac{(1-f)(R_p - R_S)}{fR_S(R_p+1)}\right)}$	*(11)*

4.3 Open system approach

In an open system like a flow-through reactor or chemostat, substrate continuously enters and exits the system, thereby drawing on an infinite substrate pool with constant isotopic composition. In this model, a small amount of the infinite substrate pool enters the reaction system and passes over into a product pool or a residual substrate pool, both of which exit the system and isotope ratios are calculated as given in equations (12) and (13) (Fry, 2006):

$R_s = R_{s,0} * \left(\frac{1-f}{\alpha_{p/s}} + f\right)$	*(12)*
$R_p = R_{s,0} * \left(1 - f + f * \alpha_{p/s}\right)$	*(13)*

Equations (12) and (13) can be simplified to (Fry, 2006)

$\delta_s \approx \delta_{s,0} - (1-f) * \varepsilon$	*(14)*

$\delta_p \approx \delta_{s,0} + f * \varepsilon.$	(15)

Note that in equations (12) to (15) the definitions of *f*, α and ε are inverse to the cited literature and therefore the subscripts s and p are exchanged.

4.4 Models used for isotope effects

For some specific applications, for instance the determination of the isotope effect during N_2 fixation and microbial or plant NH_4^+ uptake, the isotopic fractionation factor is calculated similar to eq. (*4*) by

$\alpha_{s/p} = \frac{R_{medium}}{R_{cell}}.$	(16)

R_{medium} and R_{cell} denote the isotope ratio of the medium (N_2 or NH_4^+) and the fixed nitrogen in the plant, respectively (Delwiche and Steyn, 1970; Hoering and Ford, 1960). The adaption of eq. (10) referred to as method Δ for the uptake of a medium into cells

$\varepsilon \approx \delta_{cell} - \delta_{medium}$	(17)

was used in Macko et al. (1987), Mariotti et al. (1982b) and Yoneyama et al. (1991). For modeling of isotope effects in the open sea a vertical diffusion-advection model was applied, which calculates the vertical movement of the different N compounds and couples it with equation (*4*) (Cline and Kaplan, 1975).

4.5 Methods to derive isotope effects

All approaches to calculate isotope effects presuppose a one-step process, which implies that no preceding or subsequent reaction step changes the isotopic composition in the substrate or product, respectively. As a consequence, the investigated process either needs to be isolated by suppressing preceding or subsequent reaction steps or the utilized method needs to be robust towards the assumption of a one-step process.

Method S exclusively involves the determination of the substrate's isotopic compositions $R_{s,0}$, R_s along with f during a reaction. For this reason, this method inherently determines the isotope effect for the step from the substrate to the next product. Further reaction steps do not bias the obtained isotope effect unless the substrate is subject to a preceding reaction step. Consequently, this approach is not capable of determining the isotope effect of a reaction sequence.

For the determination of the isotope effect of reaction sequences, three different methods are commonly used. The method P requires the repeated determination of $R_{s,0}$, R_p and f. Inconsistencies such as the accumulation of an intermediate can be identified by a nonlinear relation between δ_p and $-f*\ln(f)/(1-f)$. Thus, method P is well suited for experimental setups involving confined reaction vessels in closed systems. Though method Δ is a result of closed system derivations, this method has also been applied to approximate isotope effects for flow-through or open experimental setups like a steady state reactor or chemostat (Barford et al., 1999). However, in situations in which method Δ was applied, R_{pi} was frequently approximated by R_p, which presupposes that f is approx. 1 and thus both values are similar (Mariotti et al., 1981). This assumption, however, is only valid for a short period of time and is thus questionable as no objective criterion can be derived to identify the validity of this assumption. The third approach, eq. (11), requires the simultaneous determination of both the substrate and the accumulated product in microbes or plants. This approach is probably the most demanding as both R_s and R_p need to be dynamically determined if the consistency of obtained isotope effects is to be checked by variation of f.

Common to all three approaches is the determination of isotope effects for reaction sequences with a given end product. Thus, the investigated process needs to be confined to the end product. One method used to isolate a process is the use of an inhibitor to stabilize the end product, e.g. in denitrification experiments for the multi-reaction step from NO_3^- to N_2, acetylene (C_2H_2) is often used to inhibit the

281 reduction of N_2O to N_2 (Lewicka-Szczebak et al., 2014; Toyoda et al., 2005). Alternatively, short
282 incubation periods (Snider et al., 2009) or soils with small N_2O reduction potential were used (Mathieu
283 et al., 2007). Another option for process isolation is the characterization and correction of subsequent
284 reaction steps. This has been also been done for the denitrification reaction chain NO_3^-, N_2O and N_2 for
285 which the individual isotope effects of N_2O production and reduction were extracted with a
286 mathematical model based on measurements of N_2O and N_2 fluxes (Lewicka-Szczebak et al., 2015).

287 # 5 Isotope effects in the N cycle

288 The reviewed isotope effects for N cycle processes were determined based on soil incubation studies,
289 measurements in groundwater samples and pure culture studies and employing different methods (see
290 section 4) for different ecosystem N cycling processes. For each process or process chain a
291 representative isotope effect was derived, which can be used for describing N isotope fractionation
292 processes for the major terrestrial N cycling processes. The complete dataset of reviewed isotope effects
293 used is available in supplement Table S1.

294 Statistical comparisons of isotope effects are based on the non-parametric Wilcoxon test as large
295 differences in sample size or deviation from the normal distribution were found. Test statistics were
296 calculated using R (3.1.2) (R Core Team, 2014), specifically the functions wilcox.test for two groups and
297 pairwise.wilcox.test with the Bonferroni adjustment for comparison of multiple groups and the t.test
298 and pairwise.t.test for non-normal and normal distributed groups respectively. The normal distribution
299 of groups was tested with the Shapiro-Wilk-test and normality was validated unless stated otherwise.

5.1 Fractionation processes for N_2 fixation, mineral N uptake and ammonification

5.1.1 Biological N_2 fixation (BNF)

BNF is carried out by specialized organisms which use the enzyme nitrogenase to catalyze the conversion of atmospheric N_2 to NH_3. These organisms comprise aquatic cyanobacteria (e.g. Anabaena, which can entertain symbiotic relationships with plants), free-living N_2 fixing soil bacteria (e.g. Azobacter), N_2 fixing bacteria associated with plants and N_2 fixing bacteria (e.g. Rhizobium) that form a symbiosis with plants (Fabacaea).

Isotope effects for BNF (Table S2) were mainly determined by means of pure culture studies involving *Azobacter* species (Delwiche and Steyn, 1970; Hoering and Ford, 1960; Yamazaki et al., 1987) and single other free living bacterial species (Macko et al., 1987; Minagawa and Wada, 1986). With the exception of *Azobacter indicum* (3.7±3.5 ‰; Hoering and Ford (1960)), all other reported isotope effects were weak but normal e.g. for Anabaena cyanobacteria -0.6 ‰ (Minagawa and Wada, 1986) and -2.35 ‰ (Macko et al., 1987).

The isotope effect determined for N_2 fixation by symbiotic plants are -0.7±0.3 ‰ and 1.1±0.3 ‰ in leaves and wood of Acacia, 1.8±0.3 ‰ for red clover and 1.9±0.3 ‰ for Azolla pinnata (a water fern;Figure 2), indicating a slightly inverse isotope effect (Minagawa and Wada, 1986).

On average, the isotope effects for free cultures showed a weak normal isotope effect (-1.15±1.92 ‰), which is significantly different ($p < 0.05$) from the weak inverse isotope effect of experiments involving symbiotic plants (1.03±1.20 ‰). However, as both free living bacteria and symbiotic plants are available in most ecosystems, utilization of the grand mean of the available literature values of -0.57±1.98 ‰ (median -0.7 ‰) for BNF from all studies from Table S2 appears pertinent.

5.1.2 Microbial, fungal and plant NO_3^- uptake

Isotope effects for NO_3^- uptake by free living microorganisms (-6.20±4.43 ‰) and plants (*pennisetum* and *pinus*) (-7.27±4.07 ‰) vary between -18.3 and 0 ‰ (Table S3 and Figure 2), but were not significantly different ($p > 0.71$).

Two studies found very different isotope effects for NO_3^- uptake by plants (Högberg et al., 1999; Mariotti et al., 1982b) but had in common that the isotope effect strongly decreased over time, while the plants were growing. This is explained by an increasing activity of the plants NO_3^- reductase activity during plant growth, so that NO_3^- in the plant is consumed more completely and the isotope effect decreases (Mariotti et al., 1982b).

Several studies also investigated the isotope effect associated with NO_3^- uptake in marine bacteria (Macko et al., 1987; Montoya and McCarthy, 1995; Waser et al., 1998; Yoneyama et al., 1991) and found that it was strongly dependent on the organisms studied; e. g. diatoms have much stronger isotope effects compared to flagellates (Montoya and McCarthy, 1995).

Because no significant difference between the isotope effects of NO_3^- uptake by free living microorganisms and plants were found, it appears robust to use the grand mean of -6.4±4.2 ‰ (median -5 ‰) which comprises all studies from Table S3.

5.1.3 Microbial, fungal and plant NH_4^+ uptake

The isotope effect of NH_4^+ uptake was determined in several studies for both plants (-7.5±0.94 ‰) and microorganisms (-10.2±7.94 ‰), but no significant difference ($p > 0.41$) could be found, likely due to the strong variability in the group of microorganisms. Therefore we suggest using the grand mean -9.4±6.6 ‰ (median -8.0 ‰) for NH_4^+ uptake which includes all studies from Table S4.

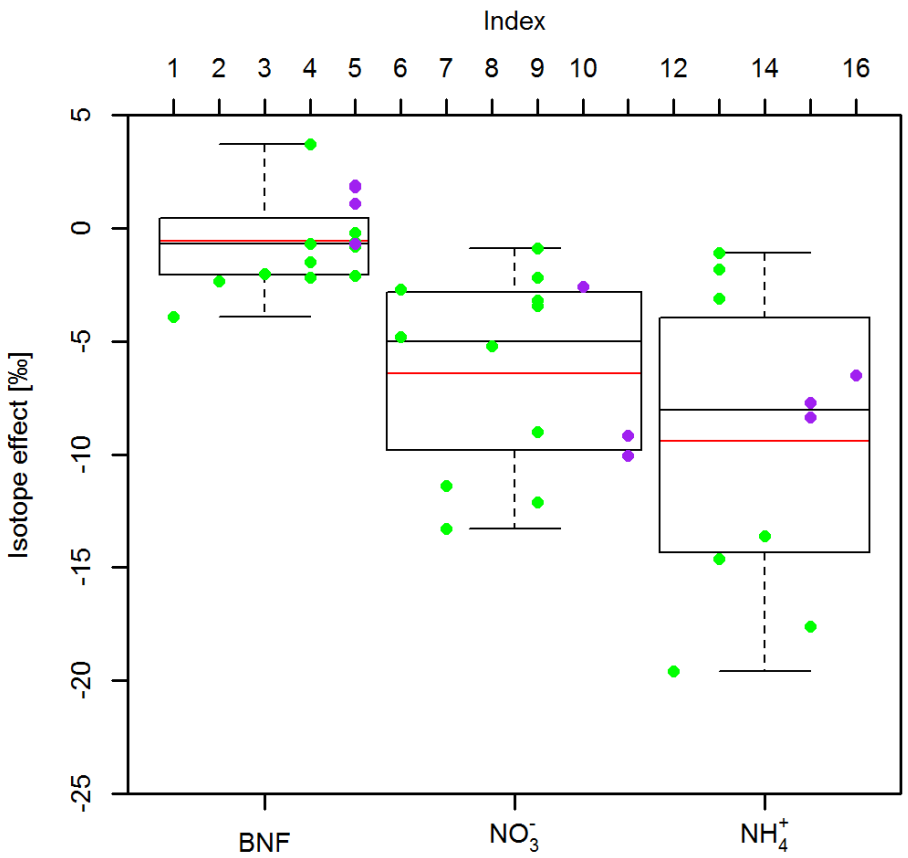

Figure 2: Boxplot of the isotope effects for BNF, NO_3^- and NH_4^+ uptake with data reported in Table S2 to Table S4. Purple dots indicate isotope effects for plants and green dots indicate pure culture studies involving free living cultures. The index numbers on the top refer to the studies in Table S2 to Table S4.

5.1.4 Ammonification

To our knowledge, only one study (Möbius, 2013) investigated the isotope effect for the process of ammonification, i.e. the mineralization of soil organic nitrogen. Values were determined for deep sea sediments (sapropels) with high organic matter content and amounted to -1.74 ‰ (-2.33 to -1.43 ‰).

5.2 Nitrification

Nitrification is the oxidation of NH_4^+ to NO_3^-. We only cover the specific type of chemo-litho-autotrophic nitrification, where ammonia is oxidized in two steps, because it is the only type represented in the reviewed literature, which investigated the conversions of (i) NH_4^+ to NO_2^-, (ii) NH_4^+ to N_2O, (iii) NH_2OH to N_2O and (iv) NO_2^- to NO_3^-. In the first step, primary nitrifiers (ammonia oxidizers) oxidize NH_4^+ to NO_2^- via

356 the intermediate NH_2OH (primary nitrification). In the following step, secondary nitrifiers (nitrite
357 oxidizers) oxidize NO_2^- to NO_3^- (secondary nitrification). During the oxidation of NH_2OH to NO_2^-, N_2O is
358 formed through chemical decomposition of NH_2OH or NO_2^- (Wrage et al., 2001).

359 Isotope effects for NH_4^+ oxidation to NO_2^- (Table S5) were determined by means of pure culture
360 experiments involving the chemoautotrophic bacteria of the genera *Nitrosomonas* and *Nitrosospira*. The
361 bacterial strain *Nitrosomonas europaea* was subject to each of the reviewed studies (N=4) revealing
362 isotope effects ranging between -38.2 and -24 ‰ with a mean of -29.9±5.1 ‰. Including reported
363 isotope effects for the other *Nitrosomonas* strains, namely *N. eutropha, N. marina* and *N.* sp.C-113a, as
364 well as *Nitrosospira tenius* leads to a slightly larger variability with values ranging between -38.2 to -14.2
365 ‰ with a mean of -27.0±7.0 ‰ (Casciotti et al., 2003; Delwiche and Steyn, 1970; Mariotti et al., 1981;
366 Yoshida, 1988). The weak isotope effects found for two marine organisms of the genus *Nitrosomonas*
367 are the main reason for the increase in variability (Casciotti et al., 2003). While the observed variability
368 for the species *Nitrosomonas europaea* may be explained by the degree of the expression of the intrinsic
369 enzymatic or diffusional isotope effects or violations of the presumption of a one-step reaction (for
370 instance accumulation of NH_2OH or N_2O), also the phylogeny of ammonia monooxygenase (AMO)
371 sequences seem to contribute to the weak isotope effects determined for *N. marina* and *N.* sp.C-113a
372 (Casciotti et al., 2003). In view of the observed dependency of isotope effects at species level, we
373 suggest to use a value of -29.6±4.9 ‰ (median -27.2 ‰) for the oxidation of NH_4^+ to NO_2^- in soils, i.e. the
374 average of the values given in Table S5, excluding the values of the marine microorganisms.

375 Compared to the isotope effect for the oxidation of NH_4^+ to NO_2^-, the isotope effect of NH_4^+ to N_2O
376 (Table S6) is strong, with a range of -64 to -46.9 ‰ (Mandernack et al., 2009; Sutka et al., 2006; Yoshida,
377 1988). Results of incubation experiments with tropical soils showed even stronger isotope effects from -
378 112 to -102 ‰ (Pérez et al., 2006). In the latter study, the $\delta^{15}N\text{-}N_2O$ values from nitrification and

379 denitrification were calculated based on an isotopic mass balance approach involving a control
380 treatment and one treatment in which nitrification and the N_2O reductase in denitrification were
381 inhibited by high concentrations (approx. 10 Vol %) of C_2H_2. In the control treatment, NO emissions were
382 six to nine times that of the C_2H_2 treatment, so that the strong isotope effect for N_2O production during
383 nitrification may have been caused by NO accumulation (Pérez et al., 2006). As a consequence, it
384 appears more robust to use a value of -56.6±7.3 ‰ (median -57 ‰) for N_2O production during
385 nitrification, including values reported by Mandernack et al. (2009), Sutka et al. (2006) and Yoshida
386 (1988).

387 The isotope effect of NH_2OH oxidation to N_2O was determined for several pure cultures and abiotic N_2O
388 production using method Δ. The measured isotope effects ranged from -26.3 to 5.7 ‰ with a mean of -
389 5.8±10.2 ‰ (Heil et al., 2014; Sutka et al., 2006, 2004, 2003). The large range in isotope effects between
390 the species *Methylococcus capsulatus*, a CH_4 oxidizing bacteria with a CH_4 mono-oxygenase also capable
391 to oxidize NH_4^+, and *Nitrosomonas europaea* in Sutka et al. (2004, 2003) is likely due to differences in
392 methanotrophic and autotropic nitrification (Sutka et al., 2003). In studies on abiotic N_2O formation,
393 different buffer media and pH values may account for the observed variability (Heil et al., 2014). In the
394 latter study, also 1:1 mixtures of NO_2^- and NH_2OH were used as a substrate and isotope effects in the
395 range of -17.8 to 0.8 ‰ were reported, which are only slightly weaker than isotope effects of NH_2OH
396 oxidation only. The isotope effects found for N_2O production during NH_2OH oxidation are weaker than
397 for N_2O production during NH_4^+ oxidation, indicating a strong isotope effect for the oxidation step from
398 NH_4^+ to NH_2OH. Using a value of -5.1±12.0 ‰ (median 0.6 ‰ and non-normal distribution (p=0.03)) for
399 NH_2OH oxidation seems robust, considering only studies from Table S7 with NH_2OH as sole substrate
400 (Heil et al., 2014; Sutka et al., 2006, 2004, 2003).

The isotope effect of the oxidation of NO_2^- to NO_3^- has so far only been described by Casciotti (2009) for a pure culture with the chemo-litho-autotrophic nitrite oxidizer *Nitrococcus mobilis*. Three experiments have been performed, in which the concentration of cells, pH and medium were varied. The incubations lasted between two and six days until the oxidation reaction was approximately completed. For all experiments inverse isotope effects were reported with a mean of 13.0±1.5 ‰ (index 12 in Figure 3). The inverse isotope effect is in agreement with calculations based on transition state theory (see Section 6) and may be caused by the formation of a strong additional N-O bond (Casciotti, 2009).

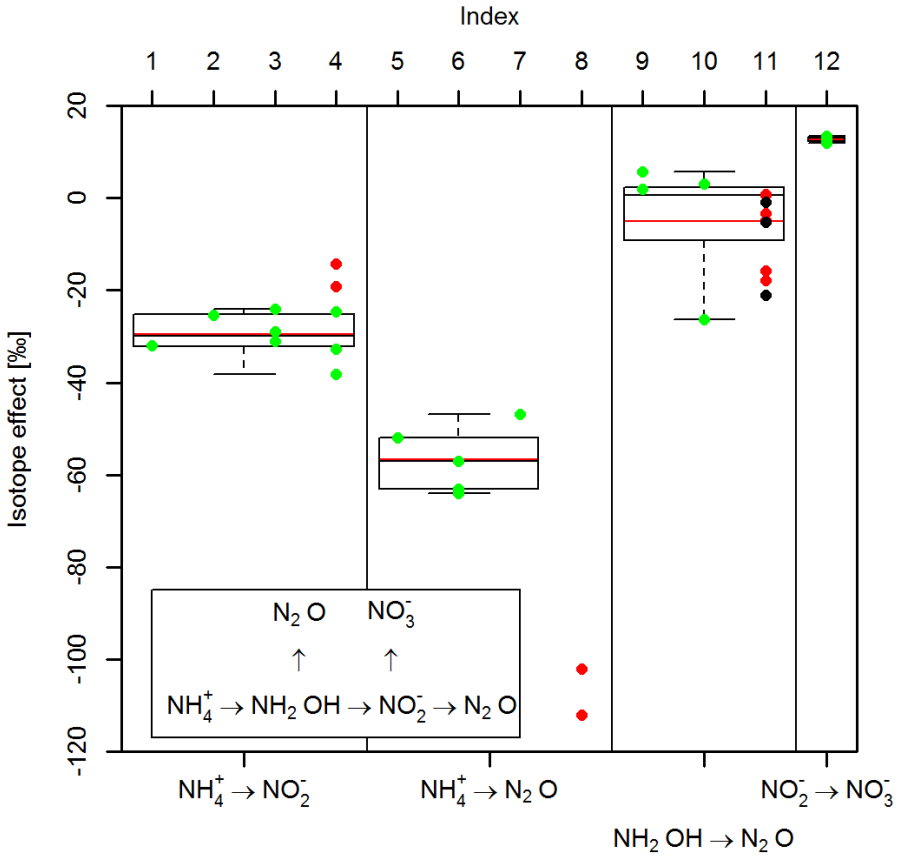

Figure 3: Boxplots of the isotope effects for the oxidation of NH_4^+ to NO_2^- reported in Table S5, the oxidation of NH_4^+ to N_2O reported in Table S6, the NH_2OH reaction to N_2O reported in Table S7 and the oxidation of NO_2^- to NO_3^-. The index numbers on the top refer to the studies in the respective tables. Green dots indicated pure culture studies, black dots abiotic reactions and the red dots are values not considered while doing boxplot calculations. The red dotted values are neglected for using aquatic organisms in study 4, having substantial NO accumulation in study 8 and using NO_2^- as additional substrate in study 12. The box on the left bottom shows all reaction path ways in nitrification reactions.

5.3 Denitrification

5.3.1 NO_3^- reduction

The first step in the denitrification process is the reduction of NO_3^- to NO_2^-. For this reaction, a variety of isotope effect studies are available comprising experiments with pure cultures as well as soil and ground water samples. The strongest isotope effects were found for pure fungal cultures (F_{PC}) with values ranging between -45.6 and -30.9 ‰ (mean: -37.8±6.6 ‰), followed by soil incubations (SI) with values ranging between -52.8 and -10 ‰ (mean: -31.4± 11.8 ‰). Isotope effects were weaker for bacterial pure culture studies (B_{PC}) with values ranging between -36.7 and -10 ‰ (mean: -25.2±8.4 ‰) and weakest for water samples (WS) ranging between -38 and -2.6 ‰ (mean: -11.4±9.5 ‰) (Table S8 and Figure 4).

While the variability of isotope effects within one experimental setup (e.g. fungal pure culture experiments) might be explained by different microbial strains (F_{PC}, B_{PC}) or a multitude of microbial organisms (SI, WS), also the isotope effects for a particular organism, e.g. *Paracoccus denitrificans* varied substantially with values ranging between -28.6 ‰ (Barford et al., 1999) and -10 ‰ (Toyoda et al., 2005). Some part of the variability between different strains may result from different enzyme structures (Casciotti et al., 2003; Rohe et al., 2014; Schmidt et al., 2004), but the large variation of values determined for a single organism indicates that the specific experimental conditions (e.g. diffusion limitation for substrate availability, accumulation of intermediates and use of C_2H_2 in experiments to block N_2O reduction) play a significant role for the determined isotope effect (Toyoda et al., 2005).

In the context of experimental conditions, the dependence of the isotope effect on temperature was investigated by Mariotti et al. (1982a, 1981), who observed a substantially weaker isotope effect for soil incubation studies at 30°C (-24.6 ‰) than at 10°C (-31.2 ‰). Weaker isotope effects are caused by increasing reaction rates at higher temperatures (Mariotti et al., 1982a) as diffusion of substrate into the cell is the rate limiting step, and the isotope effect shifts towards the weaker isotope effect associated

with diffusion. At low reaction rates, substrate delivery via diffusion is relatively higher so that the stronger enzymatic isotope effect is expressed. However, in soil incubation experiments (Snider et al., 2009) using an upland and a wetland site under different moisture and temperature conditions revealed contradicting results. Though the denitrification rates varied by more than an order of magnitude between treatments, the measured isotope effects varied by less than 9‰ and no significant difference in isotope effects was found.

Besides the effects of temperature, moisture or substrate availability on isotope effects, the effect of the added substrate's (NO_3^-) isotopic composition was investigated by utilizing NO_3^- containing ^{15}N at levels from natural abundance up to 1 atom%, i.e. approx. 1750 ‰ (Mathieu et al., 2007). Already substrate enrichment to 0.4 atom%, i.e. approx. 92 ‰, attenuated the isotope effect by 5 ‰ (Mathieu et al., 2007). Decreasing isotope effects were also observed in incubation experiments with increasing substrate consumption (Menyailo and Hungate, 2006; Toyoda et al., 2005). While this was explained by a shift of non-steady state to steady-state conditions in the considered reaction chains, the decreasing isotope effect could partly be due to complete substrate consumption within a microbial cell. This leads to decreased isotope effects as the isotope effect shifts to the weaker isotope effect of diffusion (Mariotti et al., 1982a).

Influence of the experimental design

Multiple Wilcoxon tests showed that the average isotope effect for NO_3^- reduction observed in WS was significantly weaker than the average effect of F_{PC}, B_{PC} and SI, which were not significantly different ($p > 0.18$) from each other (Figure 4).

The above classification integrates over all available calculation methods, and therefore comprises isotope effects for NO_3^- reduction to NO_2^- as well as NO_3^- reduction to N_2O. Also the direct comparison of subsets of WS (S_{WS}; η =-8.5±6.3 ‰) and SI (S_{SI}; η =-31.3±6.1 ‰), for which NO_3^- reduction to NO_2^- was

461 determined with the same approach (i.e. equations (5) and method S) revealed significantly weaker
462 isotope effects associated with WS ($p < 5*10^{-6}$).

463 Other subsets could not be compared statistically as the isotope effects for class WS (n=10) were
464 calculated according to method S, except for three studies, in which also different methods were used.
465 This consistent significant difference of class WS compared to SI, B_{PC} and F_{PC} is remarkable because WS
466 comprises subsurface, river and seawater samples. For subsurface water samples, some studies report
467 weak isotope effects between -5.2 and -2.6 ‰ (Fryar et al., 2000; Fustec et al., 1991; Mariotti et al.,
468 1988), whereas others show stronger isotope effects ranging between -19.8 and -11.0 ‰ (Böttcher et
469 al., 1990; Smith et al., 1991; Well et al., 2012). A range of -6.0 to -5.6 ‰ was measured for mixed surface
470 and subsurface water (Koba et al., 1997) and -8.9 ‰ for river water (Hinkle et al., 2001). Two
471 exceptionally strong isotope effects were reported for sea water (Cline and Kaplan, 1975), where a
472 vertical diffusion and advection model for open systems was used, and for NO_3^- reduction in water of an
473 old aquifer (Vogel et al., 1981), where a closed system equation with the isotopic composition of excess
474 nitrogen as input was used.

475 The weak isotope effect in aquatic systems compared to soils may be explained by systematic
476 differences in both environments, e.g. different microbial communities, pH values or temperature.
477 However, dead-end soil pores, in which NO_3^- may be completely consumed may explain the weak
478 isotope effects (Mariotti et al., 1988). Complete consumption of substrate in dead-end pore water does
479 not affect the isotopic composition of the substrate in the running ground water, as all substrate is
480 converted to product, but leads to a smaller residual substrate fraction *f* in the water. This
481 underestimation of *f* leads to an underestimation of the isotope effect in ground water when fitted to
482 the Rayleigh equation. In addition, the utilization of method S requires an estimate for the NO_3^- isotopic
483 composition at the initial time point ($\delta_{s,0}$). Since no initial time point and NO_3^- composition can be

484 defined for ground water, excess N_2 in the groundwater is used as a proxy for the amount of already
485 reacted NO_3^- (1-*f*) (Vogel et al., 1981), or alternatively chloride (Cl^-) is used as a normalizing, inert tracer,
486 which may contribute to the overall uncertainty of calculation of isotope effects (Koba et al., 1997).
487 However, this method does not necessarily lead to a systematic bias. Alternatively, the weak average
488 isotope effect found for ground water studies may be explained by the relation between reaction rate
489 and isotope effect. Therefore, in aquifers high reaction rates lead to weak isotope effects (Mariotti et al.,
490 1988) and slow rates to the rare strong isotope effects (Vogel et al., 1981). The weaker isotope effect in
491 aquatic systems can also be attributed to a weaker isotope effect for diffusion in water-saturated
492 compared to unsaturated soil (Well et al., 2012).

493 ***Influence of calculation method***

494 In the reviewed literature, the isotope effect of NO_3^- reduction is investigated using predominantly
495 methods S, P and Δ and the associated values are shown as classes S_{SI}, P and Δ in Figure 3 with averages
496 of -31.3±6.1 ‰, -40.3±5.2 ‰ and -28.5±12.4 ‰, respectively. Values determined by utilization of
497 method S represent the isotope effect for NO_3^- reduction to NO_2^-, whereas utilization of methods P and
498 Δ represent the isotope effect for the reduction to N_2O. The moderate standard deviations of classes S_{SI}
499 and P as well as their significantly different averages ($p<0.007$) indicate that the steps following NO_3^-
500 reduction to NO_2^-, i.e. NO_2^- reduction to NO and subsequently N_2O, also fractionate. However, no
501 significant difference of S_{SI} and class Δ could be found, most likely due to the highly variable results
502 between -52.8 ‰ (Lewicka-Szczebak et al., 2014) and -10 ‰ (Pérez et al., 2006). This indicates that
503 utilization of method Δ may be more vulnerable to uncertainties than the other methods. One source of
504 uncertainty might be the accumulation of intermediate products such as NO, which does not affect NO_3^-
505 reduction, but controls the rate of N_2O production (Pérez et al., 2006). Another source of uncertainty is
506 NO or N_2O production by nitrification and the reduction of N_2O to N_2. Incomplete suppression of N_2O

reduction to N_2 leads to an underestimation of the isotope effect due to ^{15}N enrichment in the residual N_2O. These arguments also apply to method P and may therefore not be the main reason for the large variability. Alternatively, the use of the initial isotopic composition of the substrate (NO_3^-) instead of the isotopic composition at the time of N_2O sampling can introduce an error of up to 3 ‰ even for *f* values of 0.9-0.95 (Toyoda et al., 2005). Thus, the significant difference between the classes P and Δ ($p<0.006$) might primarily be a result of the large uncertainty in the class Δ and the utilization of method Δ requires a minimization of the time difference between N_2O and NO_3^- sampling.

Influence of N_2O reductase inhibition by acetylene on the isotope effect

As outlined above, it is essential to avoid further reduction of N_2O to N_2 if methods P or Δ are applied. The suppression of the terminal denitrification step is in most cases achieved by the C_2H_2 inhibition method (Groffman et al., 2006). To investigate the effect of C_2H_2 inhibition on the derived isotope effect, two subsets were formed from class Δ, one representing experiments applying C_2H_2 ($+C_2H_2$) and one without applying C_2H_2 inhibition ($-C_2H_2$). The averages for $-C_2H_2$ and $+C_2H_2$ are significantly different ($p < 0.03$) and amount to -22.6±4.8 ‰ and -34.3±14.9 ‰, respectively. The fact that the average isotope effect for $-C_2H_2$ is weaker than the value of class S_{SI} (-31.3±6.1 ‰), which represents the first denitrification step only, confirms that N_2O reduction biases the derived isotope effect by shifting it towards weaker values (Menyailo and Hungate, 2006).

However, the average isotope effects determined for $+C_2H_2$ is substantially weaker than that of class P and is characterized by much larger variability (sd_{+C2H2} = 14.9 ‰ compared to sd_P = 5.2 ‰). The substantially weaker values observed for $+C_2H_2$ and the high variability might both be caused by incomplete inhibition of N_2O reductase during C_2H_2 incubation, as N_2O reduction can account for an increase in $\delta^{15}N\text{-}N_2O$ of up to 20 ‰ (Menyailo and Hungate, 2006). Thus, weaker isotope effects may be

biased by incomplete inhibition and the strongest isotope effects may represent the intrinsic enzymatic isotope effect found in a situation of complete inhibition.

Taking into account the above review and discussion of isotope effects, the values -8.5±6.3 ‰ (class S_{WS}; median -5.6 ‰ and non-normal distribution ($p<0.02$)) and -31.3±6.1 ‰ (class S_{SI}; median -31.2 ‰) appear reasonable for the reduction of NO_3^- to NO_2^- in aquatic and terrestrial environments, respectively (Figure 4). For the reduction of NO_3^- to N_2O, a large variety of values have been reported, in which different experimental conditions and calculation methods have been applied. A crucial point in measuring an unbiased isotope effect for NO_3^- to N_2O reduction is the complete inhibition of the N_2O reduction to N_2. Therefore, we suggest using the value -42.9±6.3 ‰ (median -44.7 ‰) including class P as well as the values -45 ‰ and lower from class Δ since for both the efficiency of inhibition was corroborated and negligible amounts of N_2O were reduced to N_2.

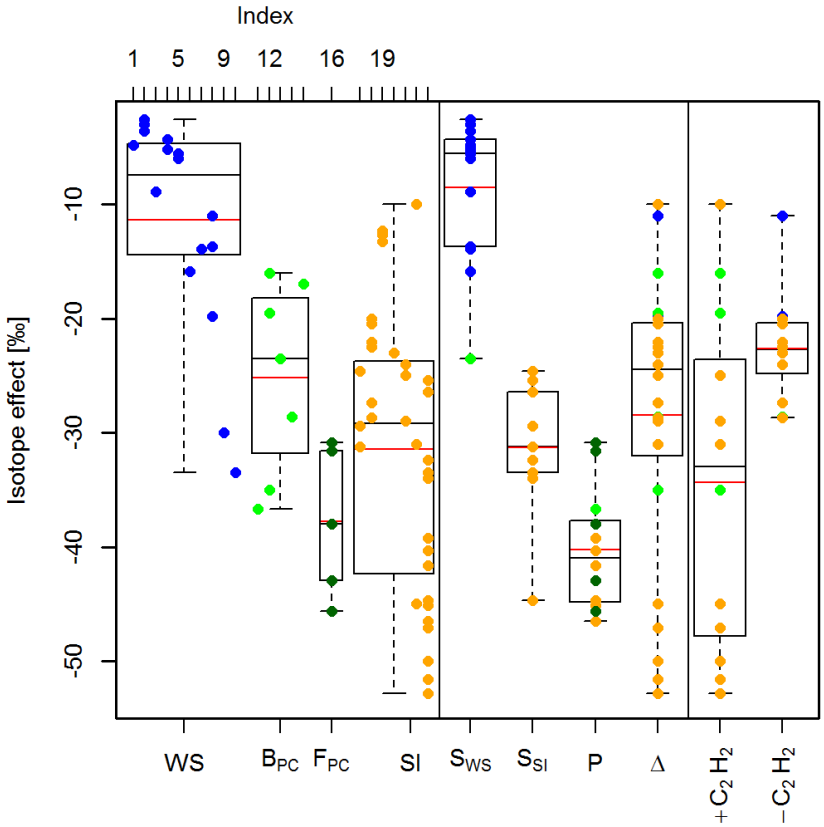

Figure 4: Boxplots of reported isotope effects for NO_3^- reduction. WS: studies on NO_3^- reduction in water samples (blue color), B_{PC}: bacterial pure culture studies (light green color), F_{PC}: fungal pure culture studies (dark green color), SI: soil incubation studies (orange color). S_{WS}: isotope effects for aquatic environments using method S, S_{SI}: soil incubations, using eqs. (5) and method S. P represents the isotope effects for NO_3^- reduction to N_2Oemploying method P. The Δ box gives the values for all studies in which method Δ was used to determine the isotope effect. The data from Δ was additionally split into studies, using C_2H_2 ($+C_2H_2$) and omitting C_2H_2 inhibition ($-C_2H_2$). The index numbers on the top identify the published studies in Table S8.

5.3.2 NO_2^- reduction

The majority of isotope effects reported in the reviewed literature are based on pure culture studies involving bacterial denitrifiers (D), which show overall weak isotope effects of -15.8 to -6.9 ‰ with a mean of -11.8±4.52 ‰, and fungal denitrifiers (FD) with isotope effects ranging from -29.3 to -6.0 ‰ with a mean value of -15.1±7.0 ‰. In contrast, NO_2^- reduction during nitrifier denitrification (class ND) resulted in a narrow range (-35.1 to -33.7 ‰) of strong isotope effects with a mean of -34.45±0.66 ‰ and the isotope effects for soil incubations (SI) were between -33.2 and -11.2 ‰ with a mean value of -21.7±6.7 ‰ (Table S9, Figure 5).

The average isotope effect of class ND was significantly different from all other classes ($p < 0.02$) while the classes D, FD and SI were not significantly different form each other ($p > 0.16$). Though there were only two studies on nitrifier denitrification, which were carried out with the same microorganism, the significant difference and strong isotope effect may indicate a stronger isotope effect of nitrifier-denitrification compared to denitrification. The large variability within class FD however may reflect the broad range of different species involved (see Table S9) and points to pronounced differences of isotope effects among the species. The large variability of isotope effects in soil incubation experiments (class SI) may reflect not only variable experimental conditions and the range between the isotope effects of diffusion and enzymatic reaction, but also a mixture of involved organisms such as nitrifiers, denitrifiers and fungi.

The magnitude of the isotope effect of NO_2^- reduction to NO, was determined by method S (-19.8±7.6 ‰) in two studies (Bryan et al., 1983; Mariotti et al., 1982a). Mariotti et al. (1982a) also investigated the effect of the reaction rate on the isotope effect for NO_2^- reduction by manipulating temperature and

568 carbon supply by addition of glucose. The isotope effects diminished with increasing reaction rate
569 because of diffusion limitation. Bryan et al. (1983) investigated the rate dependence by changing NO_2^-
570 and succinate concentration, but found stronger and weaker isotope effects with increasing rate,
571 respectively. The discrepancy between both studies was explained by the relative rates of diffusion and
572 enzymatic reactions involved, indicating that the rate alone cannot be taken as a measure of the
573 magnitude of the isotope effect without consideration of the specific mechanism.

574 The reported isotope effects for NO_2^- reduction to N_2O have been calculated by both method P (-
575 12.4±5.7 ‰) and Δ (-24.2±10.3 ‰), which are significantly different ($p<0.02$). Differences are due to the
576 involvement of class ND in the isotope effects determined by class Δ (Sutka et al., 2004, 2003; Yoshida,
577 1988). For denitrification experiments only, the isotope effects calculated by methods P and Δ (-
578 14.9±6.7 ‰) are not significantly different ($p>0.21$). However, because neither the presence of nitrifier
579 denitrification nor the presence of fungal denitrification can be excluded for terrestrial environments, all
580 values for NO_2^- reduction to N_2O from classes P and Δ are likely to be observed. The weaker isotope
581 effect of class P and class Δ without ND compared to class S points to an inverse isotope effect for the
582 NO to N_2O reduction, which is in agreement with section 5.3.3.

583 For denitrification of NO_2^- to NO the value -19.8±7.6 ‰ (median -20.5 ‰) found for class S seems to
584 reflect the variety of environmental conditions and composition of microorganisms likely to be
585 encountered in terrestrial environments. Though experimental confirmation of the strong isotope
586 effects for ND is pending, separate values for denitrification and nitrifier-denitrification may be
587 pertinent. As no significant difference between D and FD could be found, a value of -14.9±6.7 ‰
588 (median -14.0 ‰) for denitrification, comprising class P and the denitrification studies in class Δ appears
589 reasonable. Nitrifier denitrification may be treated with a value of -34.5±0.7 ‰ (median -34.5 ‰).

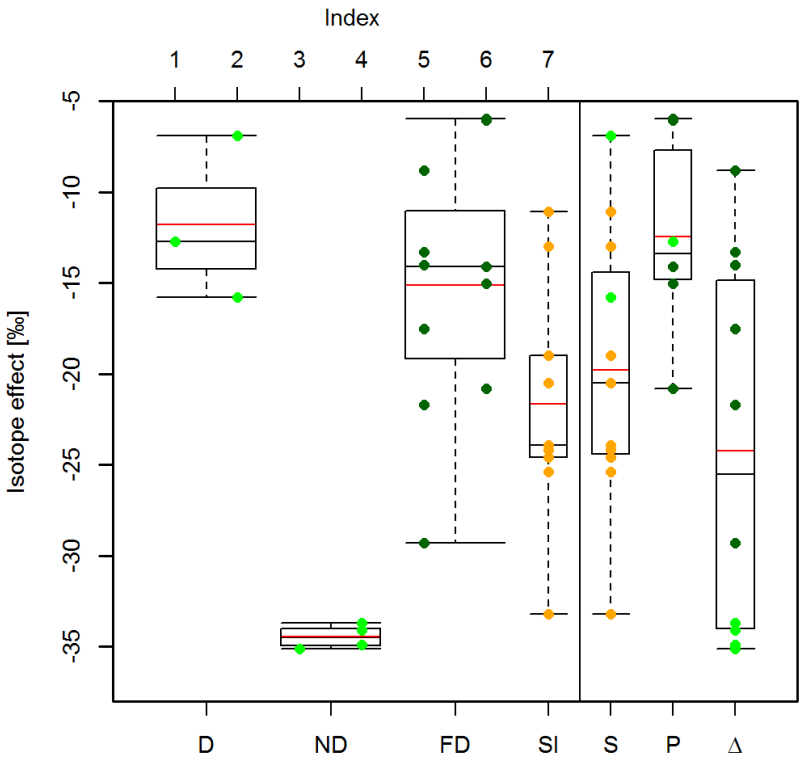

590

591 *Figure 5: Boxplots of reported isotope effects for NO_2^- reduction. D: Bacterial pure culture studies for denitrification (light green),*
592 *ND: Bacterial pure culture studies for nitrifier-denitrification (light green), FD: fungal denitrification studies (dark green), SI: soil*
593 *incubation studies (orange), S: soil incubations, for which method S was used. P: isotope effects for NO_2^- reduction to N_2O using*
594 *method P. The Δ box gives the values for all studies, where both NO_2^- substrate and N_2O product were measured and method Δ*
595 *was used to determine the isotope effect. The index numbers on the top refer to the studies in Table S9.*

596 ### 5.3.3 NO reduction to N_2O

597 The isotope effect for NO reduction to N_2O has so far only been measured for fungal denitrification
598 (Yang et al., 2014). The isotope effect was calculated by method P and was measured for both N_2O
599 isotopomers. The authors identified an inverse isotope effect with 14.0±1.6 ‰ (Yang et al., 2014), which
600 is in agreement with the findings of transition state theory discussed in section 6.

601 ### 5.3.4 N_2O reduction to N_2

602 The reviewed literature comprises both pure culture and soil incubation experiments, with isotope
603 effects ranging between -12.9 ‰ (Barford et al., 1999) to -1.8 ‰ (Ostrom et al., 2007) and an average of
604 -4.1±6.8 ‰ considering all studies (Table S10). An inverse isotope effect, i.e. ^{15}N enrichment in the

605 product N_2, was observed in flow-through incubations with open vessels and values were in the range of
606 7.6 to 16.2 ‰ (Lewicka-Szczebak et al., 2014). This inverse isotope effect might be explained by two
607 scenarios; ^{15}N depletion in N_2O during diffusion prior to reduction and/or experimental artifacts. Ostrom
608 et al. (2007) attributed normal and inverse isotope effects during N_2O reduction to two coexisting N_2O
609 reduction pathways: (1) N_2O is reduced immediately following N_2O production within the same
610 microsite or organism or (2) N_2O produced previously and released to the soil matrix is taken up and
611 reduced (Clough et al., 2005, 1999). When pathway (1) dominates, microsites or organisms may release
612 isotopically depleted N_2O. This applies if a fraction of the produced N_2O diffuses out of the cell or
613 microsite and thereby becomes depleted. With all remaining N_2O being reduced further to N_2 the N_2O
614 released to the headspace of an incubation vessel would be ^{15}N depleted compared to the initial N_2O
615 isotopic composition and application of method S results in an inverse isotope effect even though the
616 enzymatic isotope effect is a normal isotope effect. Alternatively, the determination of an inverse
617 isotope effect may be associated with artifacts caused by the experimental method. Utilization of
618 method S presumes knowledge of the N_2O isotopic composition ($\delta_{s,0}$) that was reduced to N_2. As this
619 experiment was conducted as a dynamic flow-through experiment, $\delta_{s,0}$ was determined from a parallel
620 C_2H_2 inhibition experiment. Considering the large variability of isotope effects determined for N_2O
621 production (see section 5.3.1), a weaker expressed isotope effect during N_2O production may have led
622 to enriched N_2O in the parallel C_2H_2 treatment relative to the treatment without C_2H_2 inhibition. In
623 addition, incomplete inhibition may have biased $\delta_{s,0}$ to more enriched values which would also result in
624 an inverse isotope effect. Because an inverse isotope effect has been observed so far only in a one
625 dynamic incubation experiment, and following dynamic experiments also yielded normal isotope effects
626 which ranged from -9.1 to -2.5 ‰ and were consistent with previous findings (Lewicka-Szczebak et al.,
627 2015), it appears robust to use an average isotope effect of -6.6±2.7 ‰ (median -6.8 ‰) which neglects
628 the inverse isotope effects.

5.4 Isotope site preference in N_2O

Various studies (Brenninkmeijer and Röckmann, 1999; Toyoda and Yoshida, 1999) identified site preference (SP), i.e. the difference between the $\delta^{15}N$-values for the central and terminal positions in N_2O, as a powerful tool for source partitioning of N_2O emissions because i) it is expected to be independent of the substrate isotopic composition (Toyoda et al., 2002) and ii) clear differences in SP values (Table S11 and Figure 6) could be determined for different processes involved in N_2O production (Toyoda et al., 2015). However, three issues complicate the application of this approach for source partitioning: i) the increase of SP values during N_2O reduction, i.e. the isotope effect of N_2O reduction, ii) the overlap of SP-values for fungal denitrification and nitrification (see Table S11) and iii) the variability of SP for different cultures and during the course of the reaction (Decock and Six, 2013; Yang et al., 2014). In addition, part of the inter-laboratory variability in SP values might be caused by a restricted compatibility of laboratories due to different analytical techniques and missing N_2O standards as demonstrated by Mohn et al. (2014).

The constraint (i) can be resolved in models, as the isotope effect for SP in a situation in which N_2O is reduced to N_2 has been reported to be robust within the range of -8 to -2 ‰ (Jinuntuya-Nortman et al., 2008; Lewicka-Szczebak et al., 2014; Well and Flessa, 2009). The overlap of SP values for fungal denitrification and nitrification (constraint ii) is yet unresolved, but the contribution of fungal denitrification to total N_2O emission has not yet been entirely elucidated (Maeda et al., 2015). Nevertheless, Laughlin et al. (2009) and Marusenko et al. (2013) claim the N_2O emission can be dominated by fungal denitrification in grassland and desert soils. In contrast to the narrow ranges for other processes, a large range of SP values from 15.8 to 39.9 ‰ (Maeda et al., 2015; Sutka et al., 2008) was observed for fungal denitrification. Low SP was found under acidic conditions, which favors abiotic N_2O production (Wrage et al., 2001). As abiotic N_2O formation is associated with SP of 28.4 to 35.6 ‰, increased contribution of such N_2O cannot explain a decrease in SP, so that the observed taxa-effect, i.e.

differences between bacterial and fungal N_2O production, may account for the observed variability (Maeda et al., 2015). Though experimental results (Heil et al., 2014; Toyoda et al., 2005) indicate that SP is stable during the course of a reaction, this may need further corroboration in view of an increase of SP from 15 to 29 ‰ (Yang et al., 2014) during the reduction of NO (constraint iii). Given the pending corroboration of changing SP during a reaction, the latter study was not considered in the compilation of Table S11. Though considerable variability of SP was found for fungal denitrification, the variability of SP values is smaller compared to natural abundance isotope effects of bulk ^{15}N across N transformations (see standard deviations in Table S11 for SP and chapters 5.1 to 5.3 for isotope effects). Thus, SP is more suitable for source partitioning of N_2O production, but has to go hand in hand with advances in direct denitrification measurements / N_2 measurements and an assessment of the significance of the contribution of fungal denitrification in soils.

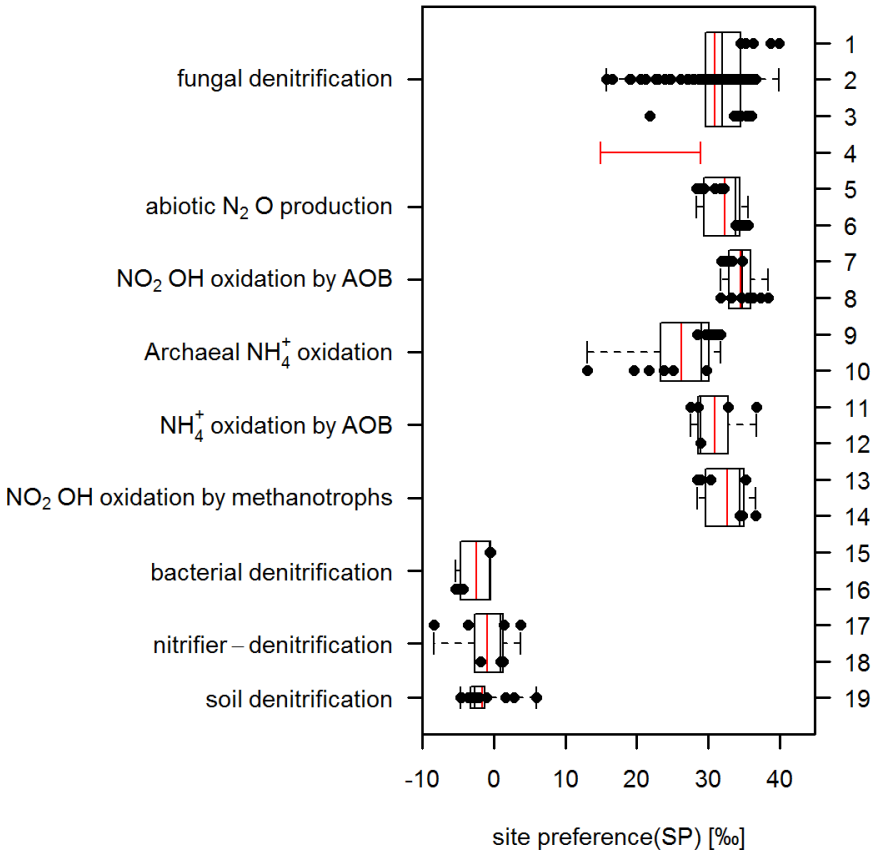

Figure 6: Boxplots of the SP values for the different N_2O producing processes. The red lines in the boxplots indicate the mean of all values in the boxplot. For study 4, the range of reported values is given by a red bar instead of single values because the measured SP values were not constant during the course of reaction. The index numbers on the right refer to the studies in Table S12.

6 Comparison with theoretical isotope effects from transition state theory

Due to the small amount of empirical information, it is pertinent to corroborate the measured isotope effects by a comparison with theoretical isotope effects, particularly for NO reduction to N_2O and NO_2^- oxidation to NO_3^-. The theoretical calculations for isotopic fractionation factors derived for equilibrium reactions are based on the idea that during a reaction the substrate molecule forms an activated complex (transition state), which decomposes to the product molecule (Bigeleisen, 1949). In thermodynamic equilibrium, the ratio of equilibrium constants for the reactions involving heavy and light isotopes, respectively, can be interpreted as the ratio of reaction rates, i.e. isotopic fractionation factor. Equilibrium constants can be derived based on the quantum mechanical partition functions which can be calculated based on spectroscopic information. Several approaches were suggested to calculate the isotopic fractionation factor, but these require additional knowledge e.g. of the effective mass of the transition state (Slater, 1948). Therefore, the isotopic fractionation factor for both NO_2^- oxidation and NO reduction was calculated according to the simplified eq. (18) for the exchange reactions given in Table 1 (Bigeleisen and Goeppert Mayer, 1947).

$$\alpha = \prod \frac{Q_{products}}{Q_{substrates}} \qquad (18)$$

The ratios of the partition functions, *Q*, for products and substrates were taken from (Begun and Fletcher, 1960) and are presented in Table 2.

Table 1: Theoretical and measured isotope effects for the exchange reactions of NO_2^- oxidation and NO reduction

Reaction	Theoretical isotope effect [‰]	Measured isotope effect [‰]	Reference

$^{15}NO_2^- + {}^{14}NO_3^- \leftrightarrow {}^{15}NO_3^- + {}^{14}NO_2^-$	65.1	13±1.5	(Casciotti, 2009)
$^{15}NO + {}^{14}N_2O \leftrightarrow {}^{14/15}N_2O + {}^{14}NO$	37.7	14±1.6	(Yang et al., 2014)

687 *Table 2: Partition function ratios used for the calculation of isotopic fractionation factors*

Molecules	Partition function ratio $^{15}Q/^{14}Q$	Temperature in Kelvin	Reference
$^{15}NO_3^-/^{14}NO_3^-$	1.1506	298.16	(Begun and Fletcher, 1960)
$^{15}NO_2^-/^{14}NO_2^-$	1.0803	298.16	(Begun and Fletcher, 1960)
$^{15}NO/^{14}NO$	1.0656	298.16	(Begun and Fletcher, 1960)
$^{14}N^{15}NO/\ ^{14}N^{14}NO$	1.1360	298.16	(Begun and Fletcher, 1960)
$^{15}N^{14}NO/\ ^{14}N^{14}NO$	1.0772	298.16	(Begun and Fletcher, 1960)

688 In agreement with the reviewed literature, the theoretical isotope effects also indicate an inverse
689 isotope effect for both reactions (Table 1). For NO_2^- oxidation to NO_3^-, a similar theoretic isotope effect
690 (58 ‰ compared to 65 ‰ in this review) was calculated in the original study (Casciotti, 2009), but both
691 theoretical values overestimate the real isotope effect. For the NO to N_2O reduction the theoretical
692 calculations exhibit a strongly inverse isotope effect with substantial ^{15}N enrichment in α-N_2O and
693 slightly inverse isotope effect for β-N_2O. These calculations agree to experimental results for $^{15}N^{\beta}$-N_2O,
694 where a strong inverse isotope effect was observed but disagree for $^{15}N^{\alpha}$-N_2O where experiments show
695 a normal isotope effect (^{15}N depletion) (Yang et al., 2014). Though the magnitude of the isotope effects
696 was overestimated by the theoretical calculations, which may be due to the simplifications in the
697 derivation of eq. (18) and the consideration of an exchange reaction, the calculated inverse isotope
698 effects support the determined inverse isotope effects for the NO_2^- oxidation and NO reduction.

699 7 Simulation approaches

700 The occurrence of N isotope fractionation during N turnover processes has been used in a number of
701 applications; for example, to reveal reaction pathways in laboratory scale experiments (Lewicka-
702 Szczebak et al., 2015, 2014), to constrain a process-based biogeochemical model (Bai and Houlton, 2009;
703 Houlton et al., 2006), or to simulate the global distribution of nitrogen isotopes in the ocean (Somes et
704 al., 2010) and in soil (Houlton et al., 2015). The transient simulation of the isotopic composition of an N

compound in an interacting system, such as the soil or the ocean, requires knowledge on isotopic fractionation factors, pool sizes of the different N compounds and the fluxes between the latter. Pool sizes and fluxes can be estimated by ecosystem process models. There are two general approaches to combine process modeling with isotopic calculations. The isotopic composition can i) be calculated on-line by the model itself or ii) off-line based on the modeled pools and fluxes. For the simulation of N isotopes in the ocean, approach i) was followed by Somes et al. (2010), whereas approach ii) was implemented for N simulations of tropical rain forests (Bai and Houlton, 2009), and in the non-equilibrium stable isotope simulator (NESIS), which was explicitly developed for the off-line coupling of ecosystem models with N isotope calculations (Rastetter et al., 2005). The second approach is more simple to implement as it avoids a complete recoding of the process model, however special care needs to be taken that the fluxes provided are gross fluxes (Rastetter et al., 2005). In addition, the parent process model may provide output at a lower time resolution than the internal calculations required for the isotope module, which may lead to a situation in which a pool size can be significantly changed. In such cases, the residual substrate fraction *f* is small which leads to large enrichments in the residual substrate and may lead to numeric instabilities. Splitting the parent model's output time step into a number of iterations based on the fluxes between pools and pool size increases the accuracy and stability of this approach (Rastetter et al., 2005).

These online and offline approaches may also be branched by the way of the pool descriptions. The pools can either be duplicated into a pool for heavy and light isotope (Rastetter et al., 2005) or isotope ratios or δ-values can be traced directly (Bai and Houlton, 2009; Somes et al., 2010). In the situation in which pools are split into heavy and light isotopes, a rate constant concept is applied to calculate fractionation, whereas open or closed system equations are applied if the model is formulated in terms of isotope ratios or δ-values. The advantage of the rate constant approach is that once the mass flow between pools are known, even multiple production or consumption steps can be calculated

simultaneously for each pool. The isotopic composition can subsequently be determined as the ratio of the pools containing the different isotopically substituted species (for instance, $^{14}N\text{-}NO_3^-$ and $^{15}N\text{-}NO_3^-$). Obviously, this concept doubles the amount of pools to be tracked. In contrast, the approach tracking the isotopic composition of a pool requires the sequential calculation for each process drawing from (fractionation) or adding to (mixing) a pool. For this reason, the latter approach is suited to be combined with a model that calculates mass fluxes between pools sequentially.

In a situation in which mixing and fractionation need to be calculated sequentially (i.e. due to the model architecture), the parameters determining the evolution of isotopic composition for both closed and open systems are the isotopic fractionation factor $\alpha_{p/s}$ and the residual fraction of substrate f. In process-oriented biogeochemical models, the amounts of reacted substrates per time step are often calculated based on reaction rate constants. Hence, the fraction f depends on the time discretization. The formalism to calculate isotopic fractionation in a transient model therefore needs to be independent of the time step chosen. Because calculations of the isotopic fractionation factor are exact when formulated in terms of isotope ratios, the effect of a refined time step on the final isotope ratio for both fractionation systems is investigated. The final isotopic composition $R_{s,f}$ originating from an initial substrate $R_{s,0}$ and a residual substrate $f=N_{s,f}/N_{s,0}$ needs to be equal to the final isotopic composition if an additional intermediate substrate R_i is introduced with $f_1=N_{s,i}/N_{s,0}$ and $f_2=N_{s,f}/N_{s,i}$ denoting the residual fractions for the intermediate steps and subscripts i and f indicate the intermediate and final state respectively. In the closed system the equation for one step is:

$R_{s,f} = R_{s,0}\, f^{(\alpha_{p/s}-1)}$	*(19)*

while with an additional intermediate step $R_i = R_{s,0} * f_1^{(\alpha_{p/s}-1)}$ and $R_{s,f} = R_i * f_2^{(\alpha_{p/s}-1)}$ it reads:

$R_{s,f} = R_{s,0}\, f_1^{(\alpha_{p/s}-1)} * f_2^{(\alpha_{p/s}-1)}$	(20)

which is equivalent to (19) as $f = f_1 * f_2$. An analogous investigation using open system equations shows that open system equations are not independent of the time step chosen. For this reason, closed system equations should be used in combination with isotope ratios.

However, the above derivation exclusively applies if consumption is the only process occurring. Because multiple processes may add to and draw from a pool and natural systems are never ideally closed, the utilization of small time steps was suggested to minimize the spatial input and output (i.e. *f* values close to 1) during a time step to avoid biases in isotopic calculations (Robinson, 2001). It is noteworthy that the differences between open and closed system calculations decrease with increasing residual substrate fraction *f*, so that adequate results can be achieved also with open system calculations if the time step is controlled appropriately (Wu et al., 2016).

For identifying the maximum time step for isotopic calculations, the deviation of calculated δ-values in a virtual pool from a reference simulation needs to be known. The virtual pool calculations need to cover the broad range of possible combinations of the share of N compound mixed into the virtual pool and the share of N compound consumed from the pool. As systems with large differences between the isotopic composition of the pool and added substrate and a strong isotope effect are most vulnerable to time discretization, the highest expected differences and isotope effects were used in the example calculations. The calculations presented here are based on an enriched pool with a δ-value of 50 ‰ and a process providing 1 to 99% of the pool size of a product with a δ-value of 0 ‰ to the pool. Subsequently, 1 to 99% of the initial pool is consumed with an isotope effect of -30 ‰. The reference simulation splits each combination of fraction mixed and consumed into 1000 sub steps.

Figure 7 shows the deviations of calculated δ-values for 1, 10, 50 and 100 sub steps relative to the reference simulation. The largest differences were observed for small residual substrate fractions *f* (i.e.

large enrichment of the substrate pool). For 50 sub steps, the largest deviation is less than 0.5 ‰. Assuming that 0.5 ‰ is a good approximation for the average analytical precision of isotopic N compounds, and because the example is on the upper boundary of realistic isotope effects of -30 ‰ and initial δ-values of 50 ‰, time steps limiting *f* to approx. 0.01 results in unbiased simulations compared to the analytical precision. In cases, where fractionation and mixing have higher rates than the initial pool size and change the isotopic composition due to very strong fractionation and mixing with much enriched sources, a larger number of iterations may be required.

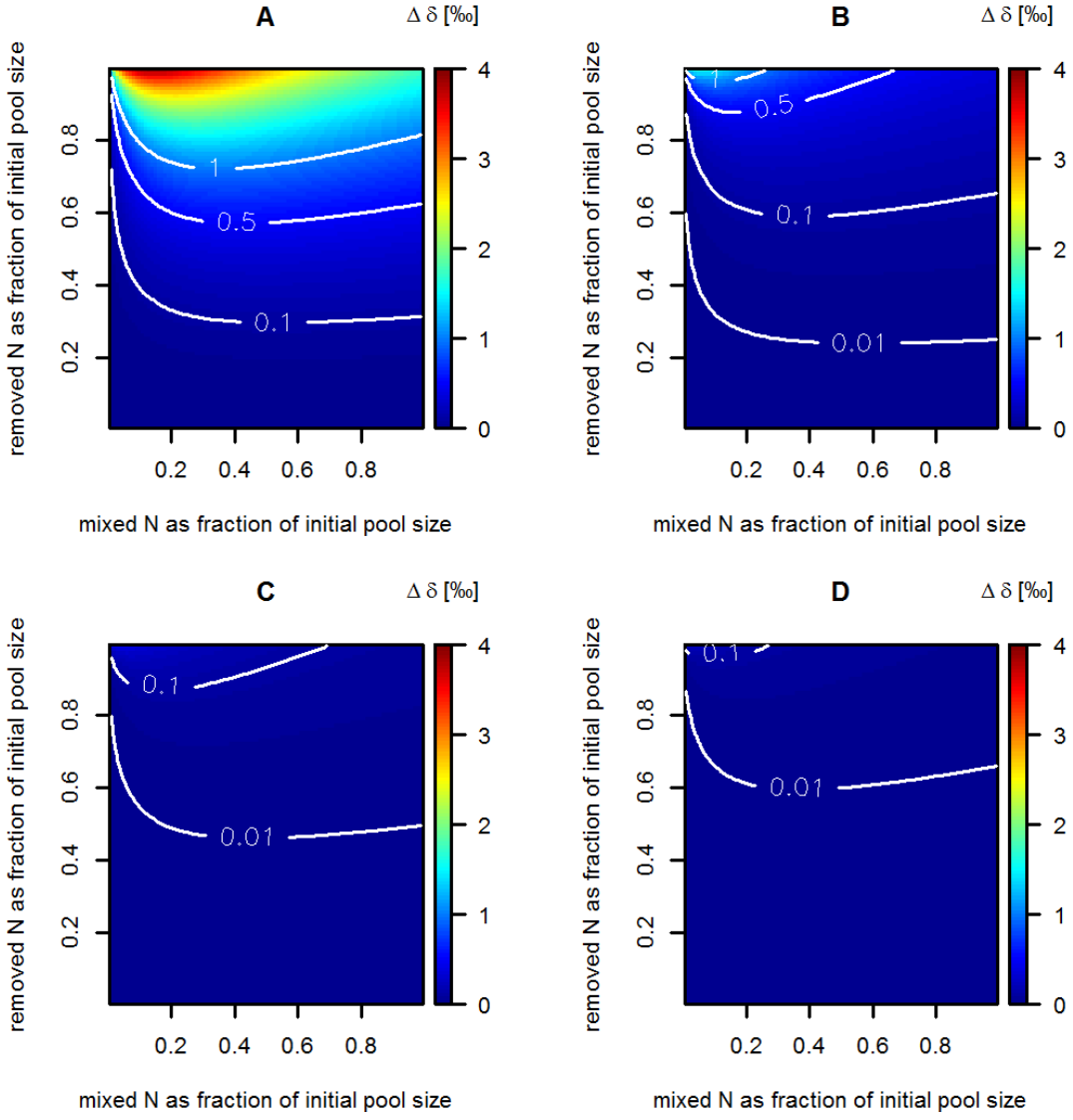

Figure 7: Deviation of simulations carried out with 1 (A), 10 (B), 50 (C) and 100 (D) sub steps from the reference simulation with 1000 sub steps. During each simulation, a compound with δ=0 ‰ is added to a virtual pool (δ=50‰) which is consumed by a virtual process (ε=-30‰). The added and consumed share ranges between 1 and 99% of the initial pool size and is split into equal parts onto every sub step. The color scheme and contour lines give the difference of δ-values between the respective simulation and the reference simulation.

8 Conclusion

The reviewed literature reveals substantial variability of isotope effects which resulted from different experimental conditions (organisms, temperature and substrate) and calculation methods. Method Δ (the difference in isotope value between the substrate and instantaneous product) showed the widest ranges of isotope effects, which may reflect the difficulty to access the ^{15}N isotopic composition of the instantaneous product. Method S (based on the isotope values of the substrate) and method P (based on the isotope values of the accumulated product) seem to yield more consistent results of isotope effects for one step reactions and reaction chains, respectively. The isotope effects determined for samples from aquatic systems, like aquifers, were weaker than in soil incubation studies. One single reason causing this difference could not be ruled out, but different microbial communities, pH values or temperature conditions and reaction rates in both systems may generally explain this difference. In addition, complete consumption in isolated dead end pores may be of special importance in aquifers.

Another general challenge for the determination of isotope effects is the isolation of a specific reaction process, so that further reaction branches do not bias the determined isotope effects. To achieve process isolation, the inhibitor C_2H_2 was used to suppress the reduction of N_2O to N_2 in the last step of denitrification. However, there is a large variability in isotope effects measured in experiments using C_2H_2, which indicates that the inhibition may not have been complete in all cases. For this reason, the complete inhibition of N_2O reduction should always be tested to make studies with C_2H_2 application more comparable.

To further constrain the isotope effects for single processes underrepresented in the literature, isotope effects were also calculated for selected processes using transition state theory. However, these calculations could confirm the sign, but not the magnitude of the isotope effect.

The suggested isotope effects and uncertainties for the N transformation processes considered in this review (see Figure 8) will form the base for isotope calculations in conjunction with biogeochemical modelling and foster the interlocking of isotope measurements and ecosystem modeling.

Modeling of the dynamic of changes of isotopic compositions for different N compounds in soils and ecosystems has been achieved by some isotope models, which are either directly implemented into or coupled to ecosystem models. Some of these models track the change of the size of ^{15}N and ^{14}N pools, whereas others calculate a δ-value for each nitrogen pool. Among the technical requirements which need to be considered when implementing isotope routines in process-based biogeochemical models, an adequate time step control for the simulated processes is crucial. Analysis of the closed and open system equations for fractionation calculations alone showed that only the closed system equations are able to obtain unbiased results when the time step is refined. However, this is only true for exclusive fractionation, whereas for multiple consecutive mixing and fractionation processes such as NO_3^- production, consumption and leaching, each of which either adding to or drawing from a pool, a relation between targeted precision and used time step has to be determined. Based on virtual pool simulations considering a) likely end member values for the strongest isotope effects, b) differences in isotopic composition between pool and added compound and c) taking into account consecutive mixing and fractionation processes, it is possible to determine the influence of the time step on the isotope signal. The simulations showed that the size of the residual fraction f is the crucial factor for producing unbiased results and f has to stay above a threshold depending on target precision, which was in our case f > 1% to reach 0.5 ‰ precision in pool δ-value with 50 iterations.. Under these conditions, the

826 application of isotope methods in process-based models will allow a more comprehensive validation and
827 further development of descriptions of nitrogen turnover processes and their interaction and
828 comparison of simulated and measured delta ^{15}N signals of e.g. N trace gas emission and N pools.
829 Specifically in the context of N_2O source partitioning, we expect that the dissemination of
830 measurements of N_2O site preference will amplify our capabilities for model validation. We consider this
831 approach a valuable contribution towards the development of tailored strategies attenuating the
832 release of harmful reactive N species.

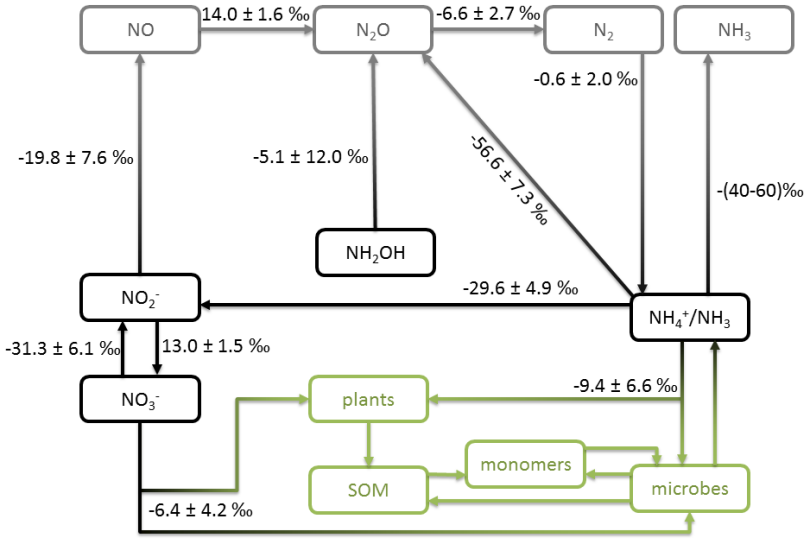

833

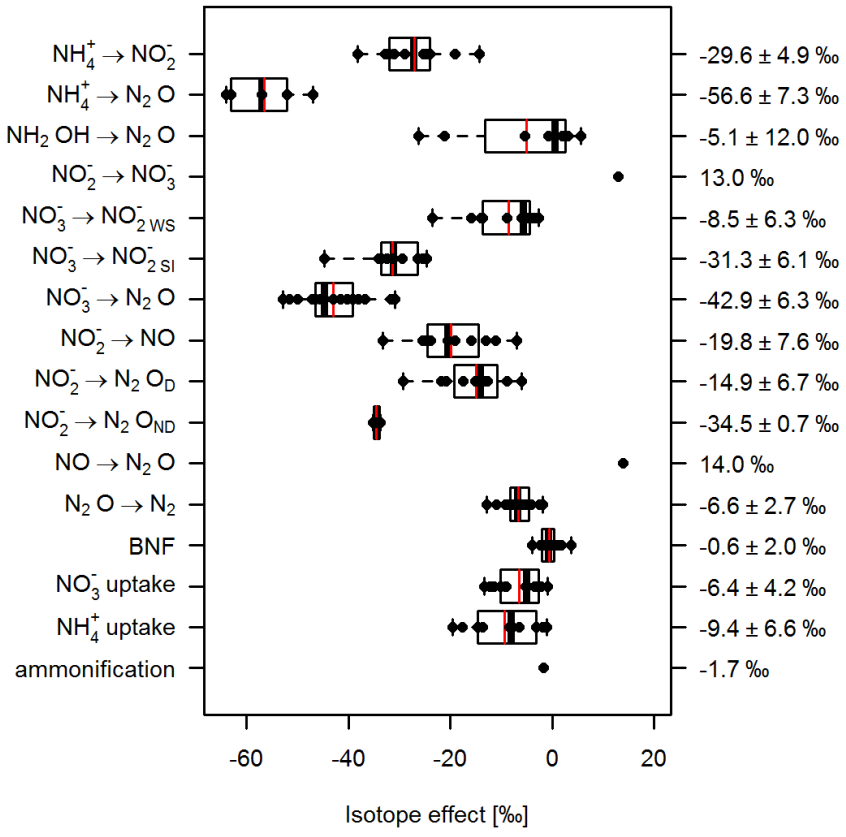

834

835 *Figure 8: Isotope effects of reviewed processes involved in terrestrial ecosystem N cycling in the upper panel. The range of*
836 *isotope effects for NH_3 volatilization was taken from* Robinson (2001)*. Boxplots for the isotope effects of reviewed processes in*
837 *the lower panel. Isotope effects were used from NH_4^+ to NO_2^-:* (Casciotti et al., 2003; Delwiche and Steyn, 1970; Mariotti et al.,
838 1981; Yoshida, 1988)*, NH_4^+ to N_2O:* (Mandernack et al., 2009; Sutka et al., 2006; Yoshida, 1988)*, NH_2OH to N_2O:* (Heil et al.,
839 2014; Sutka et al., 2006, 2004, 2003)*, NO_2^- to NO_3^-:* (Casciotti, 2009)*, NO_3^- to NO_2^- WS (water samples):* (Böttcher et al., 1990; Fryar et
840 al., 2000; Fustec et al., 1991; Granger et al., 2006; Hinkle et al., 2001; Koba et al., 1997; Mariotti et al., 1988; Smith et al., 1991;

Well et al., 2012), *NO_3^- to NO_2^- SI (soil incubations):* (Lewicka-Szczebak et al., 2015; Mariotti et al., 1982a), *NO_3^- to N_2O:* (Lewicka-Szczebak et al., 2014; Pérez et al., 2006; Rohe et al., 2014; Sutka et al., 2006), *NO_2^- to NO:* (Bryan et al., 1983; Mariotti et al., 1982a), *NO_2^- to $N_2O_{D\ (denitrification)}$:* (Rohe et al., 2014; Sutka et al., 2008, 2006), *NO_2^- to $N_2O_{ND\ (nitrifier\ denitrification)}$:* (Sutka et al., 2004, 2003; Yoshida, 1988), *NO to N_2O:* (Yang et al., 2014), *N_2O to N_2:* (Barford et al., 1999; Jinuntuya-Nortman et al., 2008; Lewicka-Szczebak et al., 2015, 2014; Menyailo and Hungate, 2006; Ostrom et al., 2007), *BNF (biological nitrogen fixation): (Delwiche and Steyn, 1970; Hoering and Ford, 1960; Macko et al., 1987; Minagawa and Wada, 1986; Yamazaki et al., 1987), NO_3^- uptake: (Högberg et al., 1999; Macko et al., 1987; Mariotti et al., 1982b; Montoya and McCarthy, 1995; Waser et al., 1998; Yoneyama et al., 1991), NH_4^+ uptake: (Delwiche and Steyn, 1970; Högberg et al., 1999; Macko et al., 1987; Waser et al., 1998; Yoneyama et al., 1991)and ammonification:* (Möbius, 2013).*The dots give used values for individual experiments and the red bars indicate the mean values.*

9 Acknowledgements

This work was supported by the German Research Foundation (DFG) [BU 1173/15-1 and LE 3367/1] and by the Swiss National Science Foundation (SNSF) [200021L_150237].

10 Bibliography

Aber, J.D., Nadelhoffer, K.J., Steudler, P., Melillo, J.M., 1989. Nitrogen Saturation in Northern Forest Ecosystems. BioScience 39, 378–386. doi:10.2307/1311067

Bai, E., Houlton, B.Z., 2009. Coupled isotopic and process-based modeling of gaseous nitrogen losses from tropical rain forests. Global Biogeochemical Cycles 23, GB2011. doi:10.1029/2008GB003361

Bai, E., Houlton, B.Z., Wang, Y.P., 2012. Isotopic identification of nitrogen hotspots across natural terrestrial ecosystems. Biogeosciences 9, 3287–3304. doi:10.5194/bg-9-3287-2012

Barford, C.C., Montoya, J.P., Altabet, M.A., Ralph, M., 1999. Steady-State Nitrogen Isotope Effects of N 2 and N 2 O Production in Paracoccus denitrificans. Applied and Environmental Microbiology 65, 989–994.

Begun, G.M., Fletcher, W.H., 1960. Partition Function Ratios for Molecules Containing Nitrogen Isotopes. The Journal of Chemical Physics 33, 1083–1085. doi:10.1063/1.1731338

Bigeleisen, J., 1949. The Relative Reaction Velocities of Isotopic Molecules. The Journal of Chemical Physics 17, 675–678. doi:10.1063/1.1747368

Bigeleisen, J., Goeppert Mayer, M., 1947. Calculation of Equilibrium Constants for Isotopic Exchange Reactions. The Journal of Chemical Physics 15, 261–267. doi:10.1063/1.1746492

Blackmer, A.M., Bremner, J.M., 1977. Nitrogen isotope discrimination in denitrification of nitrate in soils. Soil Biology and Biochemistry 9, 73–77. doi:10.1016/0038-0717(77)90040-2

Böttcher, J., Strebel, O., Voerkelius, S., Schmidt, H.-L., 1990. Using isotope fractionation of nitrate-nitrogen and nitrate-oxygen for evaluation of microbial denitrification in a sandy aquifer. Journal of Hydrology 114, 413–424. doi:10.1016/0022-1694(90)90068-9

Bremner, J.M., 1997. Sources of nitrous oxide in soils. Nutrient Cycling in Agroecosystems 49, 7–16. doi:10.1023/A:1009798022569

Brenninkmeijer, C.. A.M., Röckmann, T., 1999. Mass spectrometry of the intramolecular nitrogen isotope distribution of environmental nitrous oxide using fragment-ion analysis. Rapid Communications in

879 Mass Spectrometry 13, 2028–2033. doi:10.1002/(SICI)1097-0231(19991030)13:20<2028::AID-
880 RCM751>3.0.CO;2-J

881 Bryan, B.A., Shearer, G., Skeeters, L., Kohl, D.H., 1983. Variable expression of the nitrogen isotope effect
882 associated with denitrification of nitrite. The Journal of Biological Chemistry 258, 8613–8617.

883 Butterbach-Bahl, K., Baggs, E.M., Dannenmann, M., Kiese, R., Zechmeister-Boltenstern, S., 2013. Nitrous
884 oxide emissions from soils: how well do we understand the processes and their controls?
885 Philosophical Transactions of the Royal Society of London. Series B, Biological Sciences 368,
886 20130122. doi:10.1098/rstb.2013.0122

887 Casciotti, K.L., 2009. Inverse kinetic isotope fractionation during bacterial nitrite oxidation. Geochimica
888 et Cosmochimica Acta 73, 2061–2076. doi:10.1016/j.gca.2008.12.022

889 Casciotti, K.L., Sigman, D.M., Ward, B.B., 2003. Linking Diversity and Stable Isotope Fractionation in
890 Ammonia-Oxidizing Bacteria. Geomicrobiology Journal 20, 335–353. doi:10.1080/01490450303895

891 Cline, J.D., Kaplan, I.R., 1975. Isotopic fractionation of dissolved nitrate during denitrification in the
892 eastern tropical North Pacific Ocean. Marine Chemistry 3, 271–299. doi:doi:10.1016/0304-
893 4203(75)90009-2

894 Clough, T.J., Jarvis, S.C., Dixon, E.R., Stevens, R.J., Laughlin, R.J., Hatch, D.J., 1999. Carbon induced subsoil
895 denitrification of 15N-labelled nitrate in 1 m deep soil columns. Soil Biology and Biochemistry 31,
896 31–41. doi:10.1016/S0038-0717(98)00097-2

897 Clough, T.J., Sherlock, R.R., Rolston, D.E., 2005. A review of the movement and fate of N2O in the
898 subsoil. Nutrient Cycling in Agroecosystems 72, 3–11. doi:10.1007/s10705-004-7349-z

899 Coplen, T.B., 2011. Guidelines and recommended terms for expression of stable-isotope-ratio and gas-
900 ratio measurement results. Rapid Communications in Mass Spectrometry 25, 2538–2560.
901 doi:10.1002/rcm.5129

902 Decock, C., Six, J., 2013. How reliable is the intramolecular distribution of 15N in N2O to source partition
903 N2O emitted from soil? Soil Biology and Biochemistry 65, 114–127.
904 doi:10.1016/j.soilbio.2013.05.012

905 Del Grosso, S.J., Parton, W.J., Mosier, A.R., Ojima, D.S., Kulmala, A.E., Phongpan, S., 2000. General model
906 for N2O and N2 gas emissions from soils due to dentrification. Global Biogeochemical Cycles 14,
907 1045–1060. doi:10.1029/1999GB001225

908 Delwiche, C.C., Steyn, P.L., 1970. Nitrogen isotope fractionation in soils and microbial reactions.
909 Environmental Science & Technology 4, 929–935. doi:10.1021/es60046a004

910 Erisman, J.W., Sutton, M. a., Galloway, J., Klimont, Z., Winiwarter, W., 2008. How a century of ammonia
911 synthesis changed the world. Nature Geoscience 1, 636–639. doi:10.1038/ngeo325

912 Farquhar, G., O'Leary, M., Berry, J., 1982. On the Relationship Between Carbon Isotope Discrimination
913 and the Intercellular Carbon Dioxide Concentration in Leaves. Australian Journal of Plant
914 Physiology 9, 121–137. doi:10.1071/PP9820121

915 Farquhar, G.D., Ehleringer, J.R., Hubick, K.T., 1989. Carbon isotope discrimination and photosynthesis.
916 Annual Review of Plant Physiology and Plant Molecular Biology 40, 503–537.
917 doi:10.1146/annurev.pp.40.060189.002443

918 Fowler, D., Coyle, M., Skiba, U., Sutton, M.A., Cape, J.N., Reis, S., Sheppard, L.J., Jenkins, A., Grizzetti, B.,

Galloway, J.N., Vitousek, P., Leach, A., Bouwman, A.F., Butterbach-bahl, K., Dentener, F., Stevenson, D., Amann, M., Voss, M., 2013. The global nitrogen cycle in the twenty- first century. Phil Trans R Soc B 368, 1–13. doi:http://dx.doi.org/10.1098/rstb.2013.0164

Fry, B., 2006. Stable Isotope Ecology. Springer, New York.

Fryar, A.E., Macko, S. a., Mullican III, W.F., Romanak, K.D., Bennett, P.C., 2000. Nitrate reduction during ground-water recharge, Southern High Plains, Texas. Journal of Contaminant Hydrology 40, 335–363. doi:10.1016/S0169-7722(99)00059-5

Fustec, E., Mariotti, a., Grillo, X., Sajus, J., 1991. Nitrate removal by denitrification in alluvial ground water: Role of a former channel. Journal of Hydrology 123, 337–354. doi:10.1016/0022-1694(91)90098-3

Galloway, J.N., Aber, J.D., Erisman, J.W., Seitzinger, S.P., Howarth, R.W., Cowling, E.B., Cosby, B.J., 2003. The nitrogen cascade. Bioscience 53, 341–356. doi:10.1641/0006-3568(2003)053[0341:TNC]2.0.CO;2

Granger, J., Sigman, D.M., Prokopenko, M.G., Lehmann, M.F., Tortell, P.D., 2006. A method for nitrite removal in nitrate N and O isotope analyses. Limnology and Oceanography: Methods 4, 205–212. doi:10.4319/lom.2006.4.205

Groffman, P.M., Altabet, M.A., Böhlke, J.K., Butterbach-Bahl, K., David, M.B., Firestone, M.K., Giblin, A.E., Kana, T.M., Nielsen, L.P., Voytek, M.A., 2006. METHODS FOR MEASURING DENITRIFICATION: DIVERSE APPROACHES TO A DIFFICULT PROBLEM. Ecological Applications 16, 2091–2122. doi:10.1890/1051-0761(2006)016[2091:MFMDDA]2.0.CO;2

Haas, E., Klatt, S., Fröhlich, A., Kraft, P., Werner, C., Kiese, R., Grote, R., Breuer, L., Butterbach-Bahl, K., 2013. LandscapeDNDC: A process model for simulation of biosphere-atmosphere-hydrosphere exchange processes at site and regional scale. Landscape Ecology 28, 615–636. doi:10.1007/s10980-012-9772-x

Harris, E., Joss, A., Emmenegger, L., Kipf, M., Wolf, B., Mohn, J., Wunderlin, P., 2015. Isotopic evidence for nitrous oxide production pathways in a partial nitritation-anammox reactor. Water Research 83, 258–270. doi:10.1016/j.watres.2015.06.040

Heil, J., Wolf, B., Brüggemann, N., Emmenegger, L., Tuzson, B., Vereecken, H., Mohn, J., 2014. Site-specific 15N isotopic signatures of abiotically produced N2O. Geochimica et Cosmochimica Acta 139, 72–82. doi:10.1016/j.gca.2014.04.037

Hinkle, S.R., Duff, J.H., Triska, F.J., Laenen, a., Gates, E.B., Bencala, K.E., Wentz, D. a., Silva, S.R., 2001. Linking hyporheic flow and nitrogen cycling near the Willamette River - A large river in Oregon, USA. Journal of Hydrology 244, 157–180. doi:10.1016/S0022-1694(01)00335-3

Hoering, T.C., Ford, H.T., 1960. The Isotope Effect in the Fixation of Nitrogen by Azotobacter. Journal of American Chemical Society 82, 376–378. doi:10.1021/ja01487a031

Högberg, P., Högberg, M.N., Quist, M.E., Ekblad, A., Näsholm, T., 1999. Nitrogen isotope fractionation during nitrogen uptake by ectomycorrhizal and non-mycorrhizal Pinus sylvestris. New Phytologist 142, 569–576. doi:10.1046/j.1469-8137.1999.00404.x

Houlton, B.Z., Marklein, A.R., Bai, E., 2015. Representation of nitrogen in climate change forecasts. Nature Climate Change 5, 398–401. doi:10.1038/nclimate2538

959 Houlton, B.Z., Sigman, D.M., Hedin, L.O., 2006. Isotopic evidence for large gaseous nitrogen losses from
960 tropical rainforests. Proceedings of the National Academy of Sciences of the United States of
961 America 103, 8745–8750. doi:10.1073/pnas.0510185103

962 Jansson, P.-E., Moon, D.S., 2001. A coupled model of water, heat and mass transfer using object
963 orientation to improve flexibility and functionality. Environmental Modelling & Software 16, 37–46.
964 doi:10.1016/S1364-8152(00)00062-1

965 Jinuntuya-Nortman, M., Sutka, R.L., Ostrom, P.H., Gandhi, H., Ostrom, N.E., 2008. Isotopologue
966 fractionation during microbial reduction of N2O within soil mesocosms as a function of water-filled
967 pore space. Soil Biology and Biochemistry 40, 2273–2280. doi:10.1016/j.soilbio.2008.05.016

968 Jung, M.-Y., Well, R., Min, D., Giesemann, A., Park, S.-J., Kim, J.-G., Kim, S.-J., Rhee, S.-K., 2014. Isotopic
969 signatures of N2O produced by ammonia-oxidizing archaea from soils. The ISME Journal 8, 1115–
970 1125. doi:10.1038/ismej.2013.205

971 Kesik, M., Ambus, P., Baritz, R., Brüggemann, N., Butterbach-Bahl, K., Damm, M., Duyser, J., Horvath, L.,
972 Kiese, R., Kitzler, B., Leip, A., Li, C., Pihlatie, M., Pilegaard, K., Seufert, S., Simpson, D., Skiba, U.,
973 Smiatek, G., Vesala, T., Zechmeister-Boltenstern, S., 2005. Inventories of N2O and NO emissions
974 from European forest soils. Biogeosciences 2, 353–375. doi:10.5194/bg-2-353-2005

975 Koba, K., Tokuchi, N., Wada, E., Nakajima, T., Iwatsubo, G., 1997. Intermittent denitrification: The
976 application of a 15N natural abundance method to a forested ecosystem. Geochimica et
977 Cosmochimica Acta 61, 5043–5050. doi:10.1016/S0016-7037(97)00284-6

978 Laughlin, R.J., Rütting, T., Müller, C., Watson, C.J., Stevens, R.J., 2009. Effect of acetate on soil
979 respiration, N2O emissions and gross N transformations related to fungi and bacteria in a grassland
980 soil. Applied Soil Ecology 42, 25–30. doi:10.1016/j.apsoil.2009.01.004

981 Lewicka-Szczebak, D., Well, R., Bol, R., Gregory, A.S., Matthews, G.P., Misselbrook, T., Whalley, W.R.,
982 Cardenas, L.M., 2015. Isotope fractionation factors controlling isotopocule signatures of soil-
983 emitted N 2 O produced by denitrification processes of various rates. Rapid Communications in
984 Mass Spectrometry 29, 269–282. doi:10.1002/rcm.7102

985 Lewicka-Szczebak, D., Well, R., Köster, J.R., Fuß, R., Senbayram, M., Dittert, K., Flessa, H., 2014.
986 Experimental determinations of isotopic fractionation factors associated with N2O production and
987 reduction during denitrification in soils. Geochimica et Cosmochimica Acta 134, 55–73.
988 doi:10.1016/j.gca.2014.03.010

989 Macko, S.A., Fogel, M.L. (ESTEP), Hare, P.E., Hoering, T.C., 1987. Isotopic fractionation of nitrogen and
990 carbon in the synthesis of amino acids by microorganisms. Chemical Geology: Isotope Geoscience
991 Section 65, 79–92. doi:10.1016/0168-9622(87)90064-9

992 Maeda, K., Spor, A., Edel-Hermann, V., Heraud, C., Breuil, M.-C., Bizouard, F., Toyoda, S., Yoshida, N.,
993 Steinberg, C., Philippot, L., 2015. N2O production, a widespread trait in fungi. Scientific Reports 5,
994 9697. doi:10.1038/srep09697

995 Mandernack, K.W., Mills, C.T., Johnson, C.A., Rahn, T., Kinney, C., 2009. The δ15N and δ18O values of
996 N2O produced during the co-oxidation of ammonia by methanotrophic bacteria. Chemical Geology
997 267, 96–107. doi:10.1016/j.chemgeo.2009.06.008

998 Mariotti, A., Germon, J.C., Hubert, P., Kaiser, P., Letolle, R., Tardieux, A., Tardieux, P., 1981. Experimental
999 determination of nitrogen kinetic isotope fractionation: some principles; Illustration for the
1000 denitrification and nitrification process. Plant and Soil 62, 413–430. doi:10.1007/BF02374138

1001 Mariotti, A., Germon, J.C., Leclerc, A., 1982a. nitrogen isotope fractionation associated with the NO2-
1002 →N2O step of denitrification in soils. Canadian Journal of Soil Science 62, 227–241.
1003 doi:10.4141/cjss82-027

1004 Mariotti, A., Landreau, A., Simon, B., 1988. 15N isotope biogeochemistry and natural denitrification
1005 process in groundwater: Application to the chalk aquifer of northern France. Geochimica et
1006 Cosmochimica Acta 52, 1869–1878. doi:10.1016/0016-7037(88)90010-5

1007 Mariotti, A., Mariotti, F., Champigny, M.L., Amarger, N., Moyse, A., 1982b. Nitrogen Isotope
1008 Fractionation Associated with Nitrate Reductase Activity and Uptake of NO(3) by Pearl Millet. Plant
1009 Physiology 69, 880–884. doi:10.1104/pp.69.4.880

1010 Marusenko, Y., Huber, D.P., Hall, S.J., 2013. Fungi mediate nitrous oxide production but not ammonia
1011 oxidation in aridland soils of the southwestern US. Soil Biology and Biochemistry 63, 24–36.
1012 doi:10.1016/j.soilbio.2013.03.018

1013 Mathieu, O., Lévêque, J., Hénault, C., Ambus, P., Milloux, M.-J., Andreux, F., 2007. Influence of 15N
1014 enrichement on the net isotopic fractionation factor during the reduction of nitrate to nitrous
1015 oxide in soil. Rapid Communications in Mass Spectrometry 21, 1447–1451.

1016 Menyailo, O. V., Hungate, B. a., 2006. Stable isotope discrimination during soil denitrification:
1017 Production and consumption of nitrous oxide. Global Biogeochemical Cycles 20, GB3025.
1018 doi:10.1029/2005GB002527

1019 Minagawa, M., Wada, E., 1986. Nitrogen isotope ratios of red tide organisms in the East China Sea: A
1020 characterization of biological nitrogen fixation. Marine Chemistry 19, 245–259. doi:10.1016/0304-
1021 4203(86)90026-5

1022 Möbius, J., 2013. Isotope fractionation during nitrogen remineralization (ammonification): Implications
1023 for nitrogen isotope biogeochemistry. Geochimica et Cosmochimica Acta 105, 422–432.
1024 doi:10.1016/j.gca.2012.11.048

1025 Mohn, J., Tuzson, B., Manninen, A., Yoshida, N., Toyoda, S., Brand, W.A., Emmenegger, L., 2012. Site
1026 selective real-time measurements of atmospheric N2O isotopomers by laser spectroscopy.
1027 Atmospheric Measurement Techniques 5, 1601–1609. doi:10.5194/amt-5-1601-2012

1028 Mohn, J., Wolf, B., Toyoda, S., Lin, C.-T., Liang, M.-C., Brüggemann, N., Wissel, H., Steiker, A.E.,
1029 Dyckmans, J., Szwec, L., Ostrom, N.E., Casciotti, K.L., Forbes, M., Giesemann, A., Well, R., Doucett,
1030 R.R., Yarnes, C.T., Ridley, A.R., Kaiser, J., Yoshida, N., 2014. Interlaboratory assessment of nitrous
1031 oxide isotopomer analysis by isotope ratio mass spectrometry and laser spectroscopy: Current
1032 status and perspectives. Rapid Communications in Mass Spectrometry 28, 1995–2007.
1033 doi:10.1002/rcm.6982

1034 Molina-Herrera, S., Haas, E., Klatt, S., Kraus, D., Augustin, J., Magliulo, V., Tallec, T., Ceschia, E., Ammann,
1035 C., Loubet, B., Skiba, U., Jones, S., Brümmer, C., Butterbach-Bahl, K., Kiese, R., 2016. A modeling
1036 study on mitigation of N2O emissions and NO3 leaching at different agricultural sites across Europe
1037 using LandscapeDNDC. Science of The Total Environment 553, 128–140.
1038 doi:10.1016/j.scitotenv.2015.12.099

1039 Montoya, J.P., McCarthy, J.J., 1995. Isotopic Fractionation During Nitrate Uptake by Phytoplankton
1040 Grown in Continuous-Culture. Journal of Plankton Research 17, 439–464.
1041 doi:10.1093/plankt/17.3.439

1042 Ostrom, N.E., Ostrom, P.H., 2011. The Isotopomers of Nitrous Oxide: Analytical Considerations and

1043 Application to Resolution of Microbial Production Pathways, in: Handbook of Environmental
1044 Isotope Geochemistry. Springer Berlin Heidelberg, Berlin, Heidelberg, pp. 453–476.
1045 doi:10.1007/978-3-642-10637-8_23

1046 Ostrom, N.E., Pitt, A., Sutka, R., Ostrom, P.H., Grandy, A.S., Huizinga, K.M., Robertson, G.P., 2007.
1047 Isotopologue effects during N2O reduction in soils and in pure cultures of denitrifiers. Journal of
1048 Geophysical Research: Biogeosciences 112, 1–12. doi:10.1029/2006JG000287

1049 Pérez, T., Garcia-Montiel, D., Trumbore, S., Tyler, S., de Camargo, P., Moreira, M., Piccolo, M., Cerri, C.,
1050 2006. Nitrous oxide nitrification and denitrification 15N enrichment factors from Amazon forest
1051 soils. Ecological Applications 16, 2153–2167. doi:doi:10.1890/1051-
1052 0761(2006)016[2153:NONADN]2.0.CO;2

1053 R Core Team, 2014. R: A Language and Environment for Statistical Computing, R Foundation for
1054 Statistical Computing. Vienna, Austria. doi:10.1007/978-3-540-74686-7

1055 Rastetter, E.B., Kwiatkowski, B.L., McKane, R.B., 2005. A stable isotope simulator that can be coupled to
1056 existing mass balance models. Ecological Applications 15, 1772–1782. doi:10.1890/04-0643

1057 Riedo, M., Grub, A., Rosset, M., Fuhrer, J., 1998. A pasture simulation model for dry matter production,
1058 and fluxes of carbon, nitrogen, water and energy. Ecological Modelling 105, 141–183.

1059 Robinson, D., 2001. δ 15 N as an integrator of the nitrogen. Trends in Ecology & Evolution 16, 153–162.
1060 doi:10.1016/s0169-5347(00)02098-x

1061 Rohe, L., Anderson, T.-H., Braker, G., Flessa, H., Giesemann, A., Lewicka-Szczebak, D., Wrage-Mönnig, N.,
1062 Well, R., 2014. Dual isotope and isotopomer signatures of nitrous oxide from fungal denitrification
1063 - a pure culture study. Rapid Communications in Mass Spectrometry 28, 1893–1903.
1064 doi:10.1002/rcm.6975

1065 Santoro, A.E., Buchwald, C., McIlvin, M.R., Casciotti, K.L., 2011. Isotopic signature of N(2)O produced by
1066 marine ammonia-oxidizing archaea. Science 333, 1282–1285. doi:10.1126/science.1208239

1067 Schimel, J.P., Bennett, J., 2004. Nitrogen mineralization: Challenges of a changing paradigm. Ecology.
1068 doi:10.1890/03-8002

1069 Schmidt, H.-L., Werner, R.A., Yoshida, N., Well, R., 2004. Is the isotopic composition of nitrous oxide an
1070 indicator for its origin from nitrification or denitrification? A theoretical approach from referred
1071 data and microbiological and enzyme kinetic aspects. Rapid Communications in Mass
1072 Spectrometry : RCM 18, 2036–40. doi:10.1002/rcm.1586

1073 Slater, N.B., 1948. Aspects of a Theory of Unimolecular Reaction Rates. Proceedings of the Royal of
1074 London. Series A. Mathematical and Physical Sciences 194, 112–131. doi:10.1098/rspa.1948.0069

1075 Smith, R.L., Howes, B.L., Duff, J.H., 1991. Denitrification in nitrate-contaminated groundwater:
1076 Occurrence in steep vertical geochemical gradients. Geochimica et Cosmochimica Acta 55, 1815–
1077 1825. doi:10.1016/0016-7037(91)90026-2

1078 Snider, D.M., Schiff, S.L., Spoelstra, J., 2009. 15N/14N and 18O/16O stable isotope ratios of nitrous oxide
1079 produced during denitrification in temperate forest soils. Geochimica et Cosmochimica Acta 73,
1080 877–888. doi:10.1016/j.gca.2008.11.004

1081 Somes, C.J., Schmittner, A., Galbraith, E.D., Lehmann, M.F., Altabet, M.A., Montoya, J.P., Letelier, R.M.,
1082 Mix, A.C., Bourbonnais, A., Eby, M., 2010. Simulating the global distribution of nitrogen isotopes in

1083 the ocean. Global Biogeochemical Cycles 24, 1–16. doi:10.1029/2009GB003767

1084 Stange, C.F., Spott, O., Apelt, B., Russow, R.W.B., 2007. Automated and rapid online determination of
1085 15N abundance and concentration of ammonium, nitrite, or nitrate in aqueous samples by the
1086 SPINMAS technique. Isotopes Environ Health Studies 43, 227–236.
1087 doi:10.1080/10256010701550658

1088 Sutka, R.L., Adams, G.C., Ostrom, N.E., Ostrom, P.H., 2008. Isotopologue fractionation during N2O
1089 production by fungal denitrification. Rapid Communications in Mass Spectrometry 22, 3989–3996.
1090 doi:10.1002/rcm

1091 Sutka, R.L., Ostrom, N.E., Ostrom, P.H., Breznak, J. a, Gandhi, H., Pitt, a J., Li, F., 2006. Distinguishing
1092 Nitrous Oxide Production from Nitrification and Denitrification on the Basis of Isotopomer
1093 Abundances Distinguishing Nitrous Oxide Production from Nitrification and Denitrification on the
1094 Basis of Isotopomer Abundances. Applied and Environmental Microbiology 72, 638–644.
1095 doi:10.1128/AEM.72.1.638

1096 Sutka, R.L., Ostrom, N.E., Ostrom, P.H., Gandhi, H., Breznak, J. a, 2004. Nitrogen Isotopomer site
1097 prefeence of N2O produced by Nitrosomas europaea and Methylococus capsulatus Bath. Rapid
1098 Communications in Mass Spectrometry 18, 1411–1412. doi:10.1002/rcm.1482

1099 Sutka, R.L., Ostrom, N.E., Ostrom, P.H., Gandhi, H., Breznak, J. a., 2003. Nitrogen isotopomer site
1100 preference of N2O produced by Nitrosomonas europaea and Methylococcus capsulatus bath.
1101 Rapid Communications in Mass Spectrometry 17, 738–745. doi:10.1002/rcm.968

1102 Tong, Y.J., Yankwich, P.E., 1957. Calculation of Experimental Isotope Effects for Pseudo-First Order
1103 Irreversible Reactions. The Journal of Physical Chemistry 61, 540–543. doi:10.1021/j150551a007

1104 Toyoda, S., Mutobe, H., Yamagishi, H., Yoshida, N., Tanji, Y., 2005. Fractionation of N2O isotopomers
1105 during production by denitrifier. Soil Biology and Biochemistry 37, 1535–1545.
1106 doi:10.1016/j.soilbio.2005.01.009

1107 Toyoda, S., Yoshida, N., 1999. Determination of Nitrogen Isotopomers of Nitrous Oxide on a Modified
1108 Isotope Ratio Mass Spectrometer. Analytical Chemistry 71, 4711–4718.

1109 Toyoda, S., Yoshida, N., Koba, K., 2015. Isotopocule analysis of biologically produced nitrous oxide in
1110 various environments. Mass Spectrometry Reviews. doi:10.1002/mas

1111 Toyoda, S., Yoshida, N., Miwa, T., Matsui, Y., Yamagishi, H., Tsunogai, U., Nojiri, Y., Tsurushima, N., 2002.
1112 Production mechanism and global budget of N2O inferred from its isotopomers in the western
1113 North Pacific. Geophysical Research Letters 29, 7–1 – 7–4. doi:10.1029/2001GL014311

1114 Vitousek, P.M., Howarth, R.W., 1991. Nitrogen Limitation on Land and in the Sea : How Can It Occur ?
1115 Biogeochemistry 13, 87–115. doi:10.1007/BF00002772

1116 Vogel, J.C., Talma, a. S., Heaton, T.H.E., 1981. Gaseous nitrogen as evidence for denitrification in
1117 groundwater. Journal of Hydrology 50, 191–200. doi:10.1016/0022-1694(81)90069-X

1118 Waser, N. a. D., Harrison, P.J., Nielsen, B., Calvert, S.E., Turpin, D.H., 1998. Nitrogen isotope fractionation
1119 during the uptake and assimilation of nitrate, nitrite, ammonium, and urea by a marine diatom.
1120 Limnology and Oceanography 43, 215–224. doi:10.4319/lo.1998.43.2.0215

1121 Well, R., Eschenbach, W., Flessa, H., von der Heide, C., Weymann, D., 2012. Are dual isotope and
1122 isotopomer ratios of N 2O useful indicators for N 2O turnover during denitrification in nitrate-

contaminated aquifers? Geochimica et Cosmochimica Acta 90, 265–282. doi:10.1016/j.gca.2012.04.045

Well, R., Flessa, H., 2009. Isotopologue enrichment factors of N2O reduction in soils. Rapid Communications in Mass Spectrometry 23, 2996–3002. doi:10.1002/rcm.4216

Wolf, B., Merbold, L., Decock, C., Tuzson, B., Harris, E., Six, J., Emmenegger, L., Mohn, J., 2015. First on-line isotopic characterization of N2O above intensively managed grassland. Biogeosciences 12, 2517–2531. doi:10.5194/bg-12-2517-2015

Wrage, N., Velthof, G.L., Van Beusichem, M.L., Oenema, O., 2001. Role of nitrifier denitrification in the production of nitrous oxide. Soil Biology and Biochemistry 33, 1723–1732. doi:10.1016/S0038-0717(01)00096-7

Wu, D., Köster, J.R., Cárdenas, L.M., Brüggemann, N., Lewicka-Szczebak, D., Bol, R., 2016. N_2O source partitioning in soils using ^{15}N site preference values corrected for the N_2O reduction effect. Rapid Communications in Mass Spectrometry 30, 620–626. doi:10.1002/rcm.7493

Yamazaki, T., Hozuki, T., Arai, K., Toyoda, S., Koba, K., Fujiwara, T., Yoshida, N., 2014. Isotopomeric characterization of nitrous oxide produced by reaction of enzymes extracted from nitrifying and denitrifying bacteria. Biogeosciences 11, 2679–2689. doi:10.5194/bg-11-2679-2014

Yamazaki, T., Yoshida, N., Wada, E., Matsuo, S., 1987. N2O Reduction by Azotobacter vinelandii with Emphasis on Kinetic Nitrogen Isotope Effects. Plant and Cell Physiology 28, 263–271.

Yang, H., Gandhi, H., Ostrom, N.E., Hegg, E.L., 2014. Isotopic Fractionation by a Fungal P450 Nitric Oxide Reductase during the Production of N 2 O. Environmental Science & Technology 48, 10707–10715. doi:10.1021/es501912d

Yoneyama, T., Omata, T., Nakata, S., Yazaki, J., 1991. Fractionation of nitrogen isotopes during the uptake and assimilation of ammonia by plants. Plant and Cell Physiology 32, 1211–1217.

Yoshida, N., 1988. 15N-depleted N2O as a product of nitrification. Nature. doi:10.1038/335528a0

Zaehle, S., Friend, a. D., 2010. Carbon and nitrogen cycle dynamics in the O-CN land surface model: 1. Model description, site-scale evaluation, and sensitivity to parameter estimates. Global Biogeochemical Cycles 24, 1–13. doi:10.1029/2009GB003521

Zaehle, S., Friend, a. D., Friedlingstein, P., Dentener, F., Peylin, P., Schulz, M., 2010. Carbon and nitrogen cycle dynamics in the O-CN land surface model: 2. Role of the nitrogen cycle in the historical terrestrial carbon balance. Global Biogeochemical Cycles 24, 1–14. doi:10.1029/2009GB003522